Universidad de Oviedo

ESCUELA POLITÉCNICA DE INGENIERÍA DE GIJÓN

GRADO EN INGENIERÍA MECÁNICA

ÁREA DE MECÁNICA DE LOS MEDIOS CONTÍNUOS Y TEORÍA DE ESTRUCTURAS

ANÁLISIS POR ELEMENTOS FINITOS DEL PROCESO DE FRACTURA EN COMPONENTES METÁLICOS

D. GARCÍA-MAURIÑO REY, Luis Eloy
TUTOR: D. ª BETEGÓN BIEMPICA, María Covadonga

FECHA: Julio, 2022

ABSTRACT

This paper is focused on the analysis of fracture mechanics in metallic materials through the finite element method. We shall use a software called Abaqus and subroutines that enhance it to experiment the plastic deformation process in a Small Punch Test (SPT) and compare it to experimental results.

This study will take a deeper focus at the phenomenon known as strain gradient plasticity, which consists on the hardening experienced when considering the size effect on small specimens and it´s demonstration will be the main objective of this work. In order to do this, a model of the before mentioned SPT will be developed from scratch, an UMAT (User Material) subroutine will be implemented and the effect of size in stress-strain graphs will be evaluated and then compared it to experimental data obtained in the laboratory.

This work consists of three theoretical chapters, one chapter focused in the simulation and the results obtained and a chapter on conclusions.

INDEX

LIST OF FIGURES

CHAPTER 1

Crystalline metallic structures

During this first chapter an understanding of the basic structure of metals will be developed, likewise, the defects that can be found in this basic structure will be explained. The main reason for this is that, as we will see later, defects existing in a crystal structure will play an important role when developing the topic of plastic deformation.

Besides this, a brief explanation on the work hardening will be provided and the fracture mechanism will be explained hoping the reader will get an idea of the different mechanics in a brittle and ductile fracture. This chapter aims to be the basic foundation that sets the frame in which this work is developed.

1. 1.- MICROSTRUCTURE OF METALS

When analyzed on a microscopic scale, metals present a crystalline structure as seen in figure 1.1. This means atoms are packed in a structure in which the vicinity of each atom is equal to the next one. By studying an atom and its proximity, we can get a full vision of the whole network of atoms that compose the studied metal.

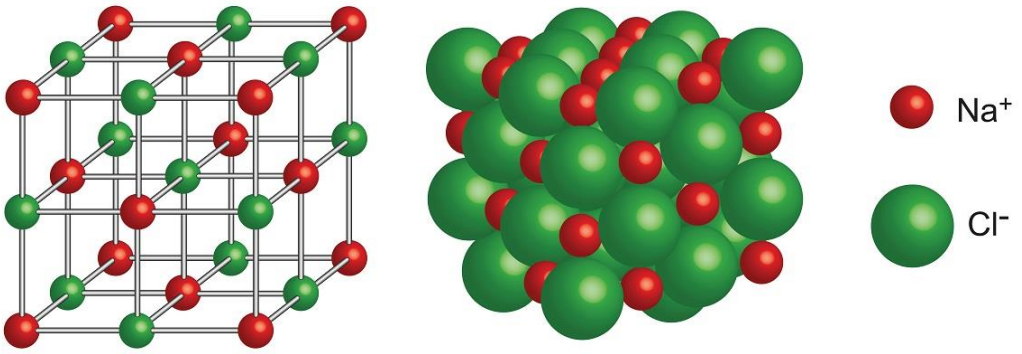

FIGURE 1.1.- Crystalline network in sodium chloride (NaCl)

It´s important to note that different metals will take different crystalline structures depending on its nature. Thankfully, most metals will take three quite simple shapes; either the hexagonal closest packed (HCP), the face-centered cubic (FCC) or the body centered cubic (BCC). Most of the commonly used metals will use either of them, for example, zinc displays an HCP structure, nickel an FCC structure and iron a BCC structure. Different examples of elements that are found in each of the structures can be seen in figure 1.2.

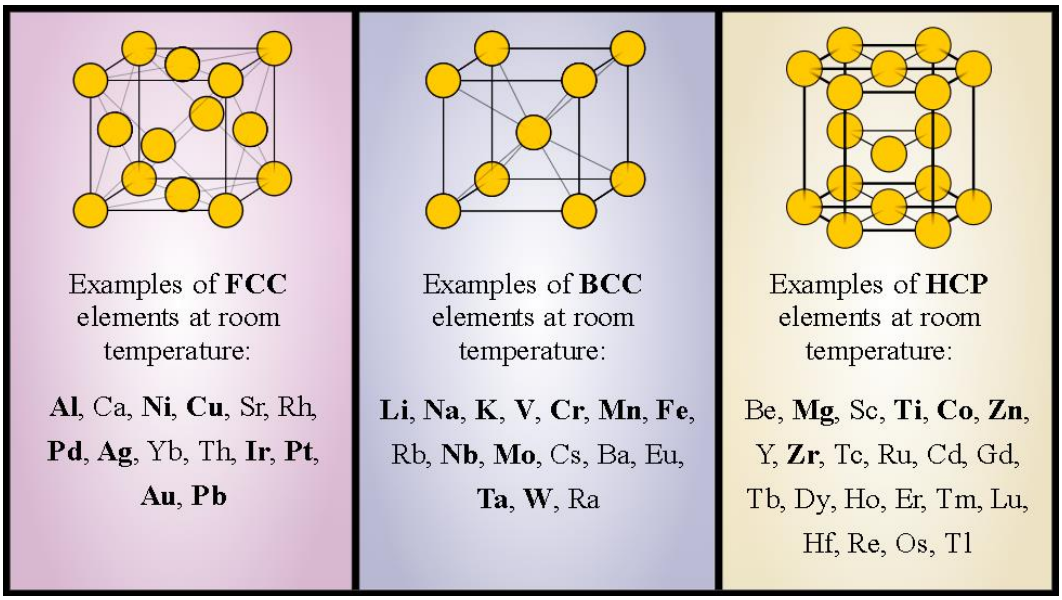

FIGURE 1.2.- FCC, BCC and HCP structures

1. 2.- DEFECTS IN THE CRYSTALINE STRUCTURE PRESENT IN METALS

Defects in crystalline structure confer the material important properties that will be of crucial importance when analyzing fracture mechanics. It´s important to stablish a clear classification of the different types of defects present on the crystalline structures. Attending to their size, we will have point defects; which exist on an atomic level, linear defects or dislocations; which affect lines of atoms, and planar defects; which are found in the interface separating two crystals.

1.2.1.- Point defects

An important detail about point defects is that they generate a stress field, which may be of much greater size than the defect itself. The defects are described in figure 1.3. and we can classify them as follows:

- **Vacancies**: When there is an atom missing in a point of the structure in which there should be one.

- **Interstitial atom**: It will happen when a foreign atom (as in, an atom that should not be found in the studied crystalline structure) or one of the atoms of the structure is found positioned interstitially.

- **Substitutional atom**: This defect is when there is a foreign atom occupying a position in the structure in which we should find an atom of the same nature as the others of the structure.

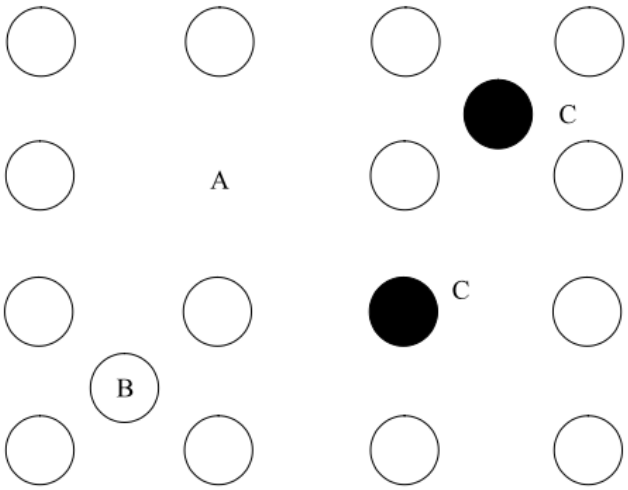

FIGURE 1.3.- Examples of vacancy (A), interstitial atom (B) and substitutional atom (C)

1.2.2.- Linear defects

As said before, linear defects affect entire lines of atoms, this kind of defect will happen during the solidification process of the metal. We can differentiate between screw dislocation and edge dislocation.

- **Screw dislocation**: When the movement of the atoms happen in a direction perpendicular to the AB line then we´ll have a screw dislocation. This is clearly visualized in figure 1.4.

- **Edge dislocation**: When the movement of the atoms happen in a direction parallel to the AB lines we´ll have an edge dislocation. This is also easier to understand looking at figure 1.4.

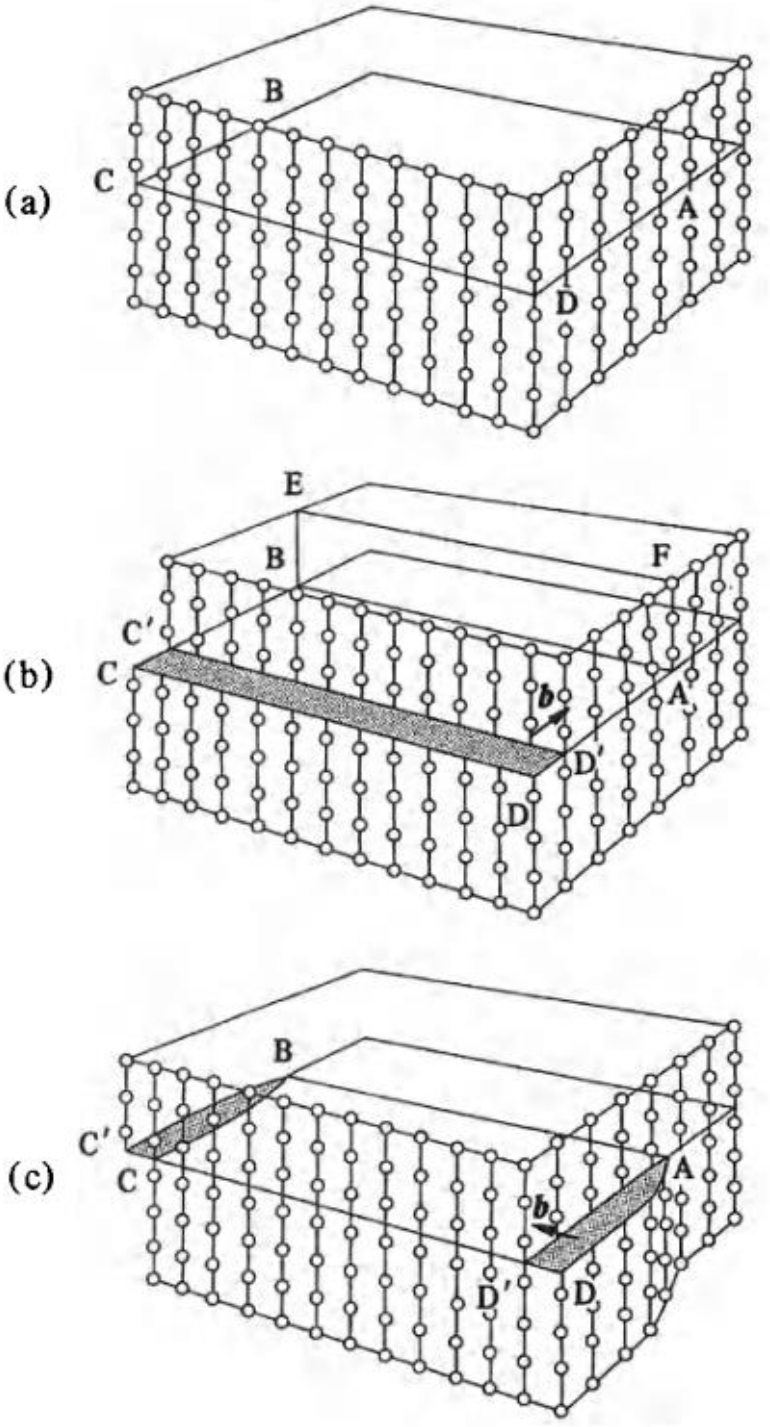

FIGURE 1.4.- Screw and edge dislocations

1. 2. 3.- Planar defects

As we know, metals are formed by small crystals as seen in figure 1.5., the regions where these crystals touch each other are called grain boundaries. It will be in these mentioned grain boundaries where planar defects are found. These defects are classified as follows:

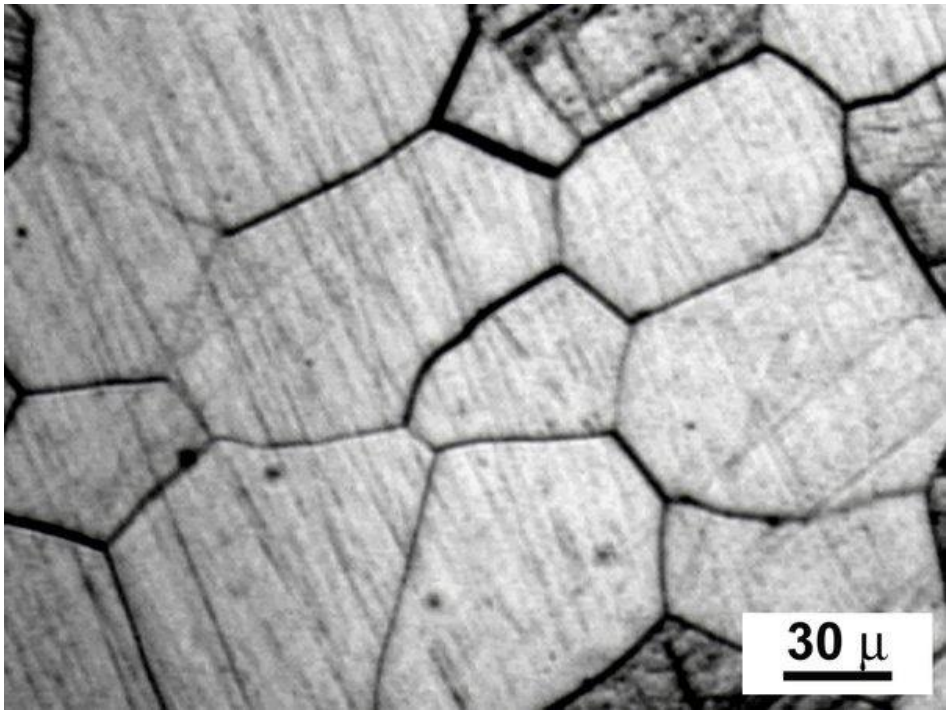

FIGURE 1.5.- Microscopic image of a metal

- **Stacking fault**: It happens when there is an abnormal sequence on the crystalline structure, for example, if we have a material with a FCC sequence of ABCABC and the sequence is altered to a ABC**BC**ABC then this is a stacking fault. This is what happens in figure 1.6.

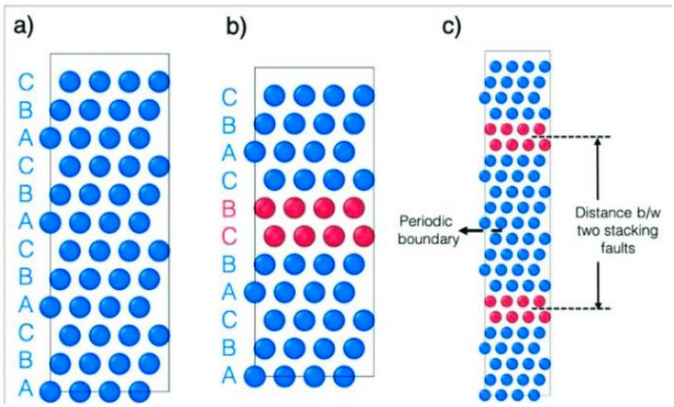

FIGURE 1.6.- Stacking fault

- **Grain Boundaries**: When the process of solidification happens the crystal growth will lead to an infinite number of small crystals being formed within the solid. The crystals will grow until meeting each other, thus the arrangement of the atoms in the grain boundaries will not be perfect.

1. 3.- HARDENING OF METALS

We regard hardening as the process in which, due to some process the material has undergone, there is an increase in the elastic limit. In order to have plastic deformation the defects mentioned in the last part come into play, the dislocations will require a minimum force to displace them, hardening will introduce obstacles that will impede these movement thus increasing the force needed for the deformation. There are different mechanics to induce hardening on a material, particularly on metals.

The first process that shall be mentioned is known as Hall-Petch method. This method relies on the increased difficulty dislocations will experience when moving due to a reduction of the grain size. When dislocations reach a grain boundary, extra stress is needed to be able to move past it. As a logical consequence, when the grains are smaller the number of them will increase and the dislocation will be forced to move past a higher number of dislocations. The final consequence is that a bigger stress will be needed for deformation.

A second process would be the precipitation hardening. In this method, the increased dislocation movement difficulty is achieved through the introduction of particles with impurity phase. The procedure to create these is based in the changes in solid solubility due to temperature.

A third and very important process is work hardening. When a metal undergoes a cold plastic deformation its number of dislocations increases, an increase in the number of dislocations inevitably leads to dislocations "crashing" and tangling to each other when trying to move through the material. The process is described in figure 1.7.

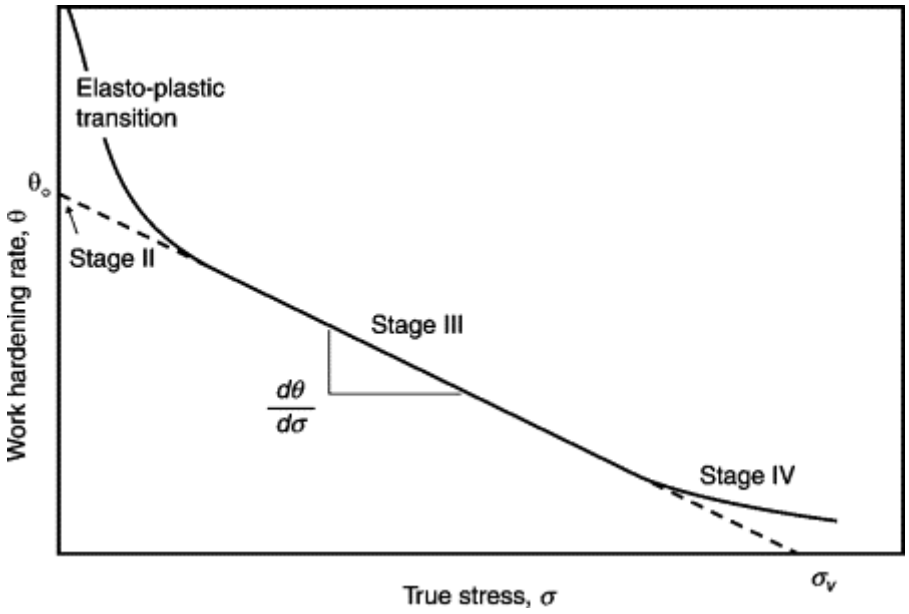

FIGURE 1.7.- Work hardening in a material

A fourth and last process for achieving hardening in a metal would be solid solution strengthening. In this process hardening is achieved by introducing atoms of one element to the crystal network of a different element, the result is a solid solution. This process is substitutionally or interstitially. The next figure 1.8. represents both situations:

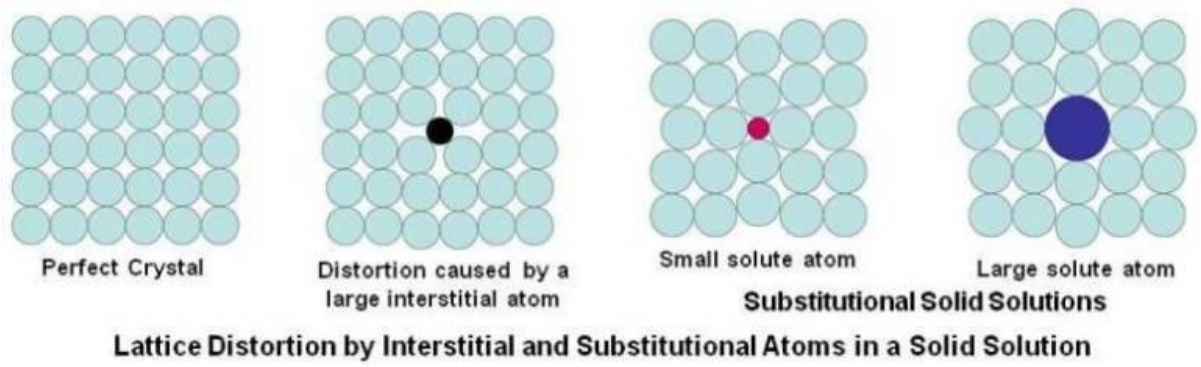

FIGURE 1.8.- Solid solution strengthening

1. 4.- FRACTURE MECHANISM

By definition, a fracture is a process in which two or more parts of the same object or material separate due to the tension produced by a force or addition of forces. Understanding fractures has long been one of the most interesting topics in engineering given that most fractures will lead to a critical failure of the system in question. We shall classify fractures in two categories: brittle and ductile fractures.

1. 4. 1.- Brittle fractures

Brittle fractures show no significant deformation of the specimen before fracture, it is sometimes described as a “clean” cut like seen in figure 1.9. It´s typical of materials such as ceramics, but not so common in metals. Commonly, brittle fracture happens when there is a breakage of the atomic bonds between the atoms of a certain plane. In metals, brittle fracture usually happens at very low temperatures, this is because when the metal suffers stress and the dislocations start moving, the nearby atoms in the crystal structure do not move because of the low temperature, this facilitates the rapid growth of cracks.

FIGURE 1.9.- Examples of brittle fractures

Griffith theory on brittle fracture states that an existing crack will grow in size when the rate of strain-energy release from the surrounding stress field is bigger than the stress that can be assimilated by the crack extension. In fracture mechanics, it´s considered that the crack will grow when the stress field around its tip achieves a certain value.

1. 4. 2.- Ductile fractures

A ductile is a fracture in which there is obvious plastic deformation before fracture. In normal conditions, it´s the most common type of fracture in metals and it´s the object of study of this work.

As we will see later, when analyzing an axial loading test, it is interesting to note than in ductile fractures the maximum load and the fracture load are different, with the fracture load being smaller. This is because the material experiences plastic deformation until the maximum load point, and then the deformation will focus on the place where the fracture happens

There are different stages that happen during a ductile fracture, the stages can be clearly visualized in figure 1.10.:

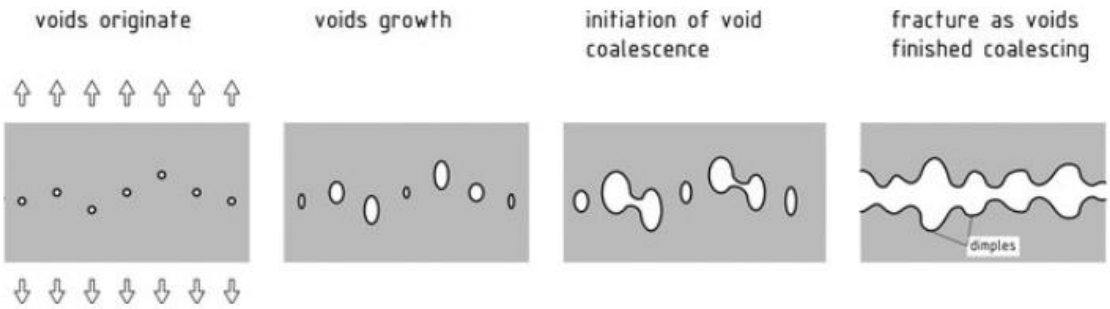

FIGURE 1.10.- Stages of ductile fracture

- **Void formation**: Voids are formed due to the tension applied and the intrinsic porosity of the material.

- **Voids growth**: As stress is applied the voids grow.

- **Void coalescence**: As the voids keep growing they eventually touch each other leading to bigger voids.

- **Fracture**: Once the voids completely grow and coalescence enough the material will be divided in two parts and we will have the fracture.

CHAPTER 2

Flow plasticity theory

Plasticity plays a crucial role on this study. As mentioned before, in a ductile fracture the material will experience noticeable plastic deformation before the fracture happens. During this chapter we will develop understanding on the flow plasticity theory.

On the first part a brief introduction to the axial deformation test and the different behaviors of ductile and brittle materials will be provided to the reader. Then, we will move on to some general topics interesting when treating the subject of flow plasticity and lastly some of the most commonly used failure criterion will be briefly introduced.

2.1.- INTRODUCTION

When a material is subjected to a certain force, part of it will deform elastically but part of it will experience permanent deformation. In many engineering's applications it is of crucial importance understanding when the deformation will stop being elastic and behave plastically. Ideally speaking, materials in service will be loaded to a point within the elastic limit and won´t experience plastic deformation. In this case, fatigue would be the determining factor on fracture, but fatigue is out of the scope of this study.

The most common test for studying the behavior of a material that´s suffering tension is the stress-strain test as in Figure 2.1. The interest of this test is that, while being relatively simple, it shows a clear picture of the behavior of a material.

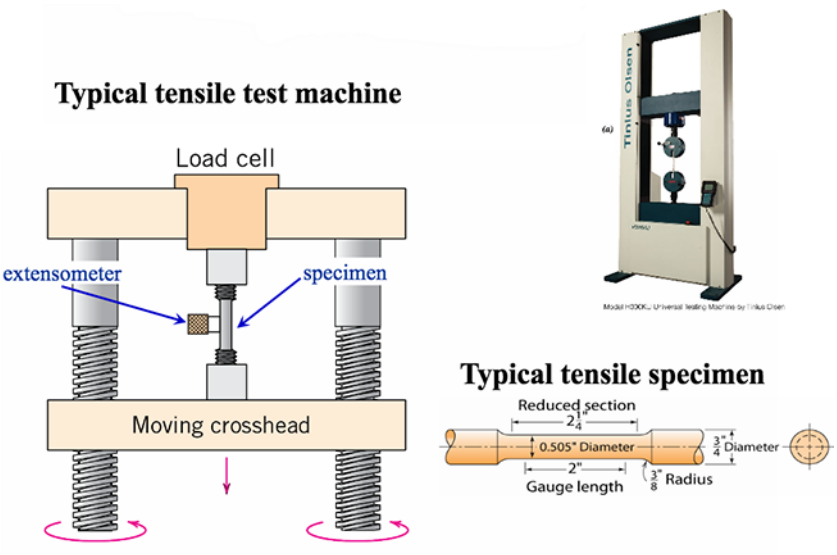

FIGURE 2.1.- Axial load test machine and specimen

During the test, a specimen will be subjected to a gradual load while the stress and strain are recorded and compared to the initial elongation and section. The results of this test in a ductile material will look as follows in Figure 2.2.:

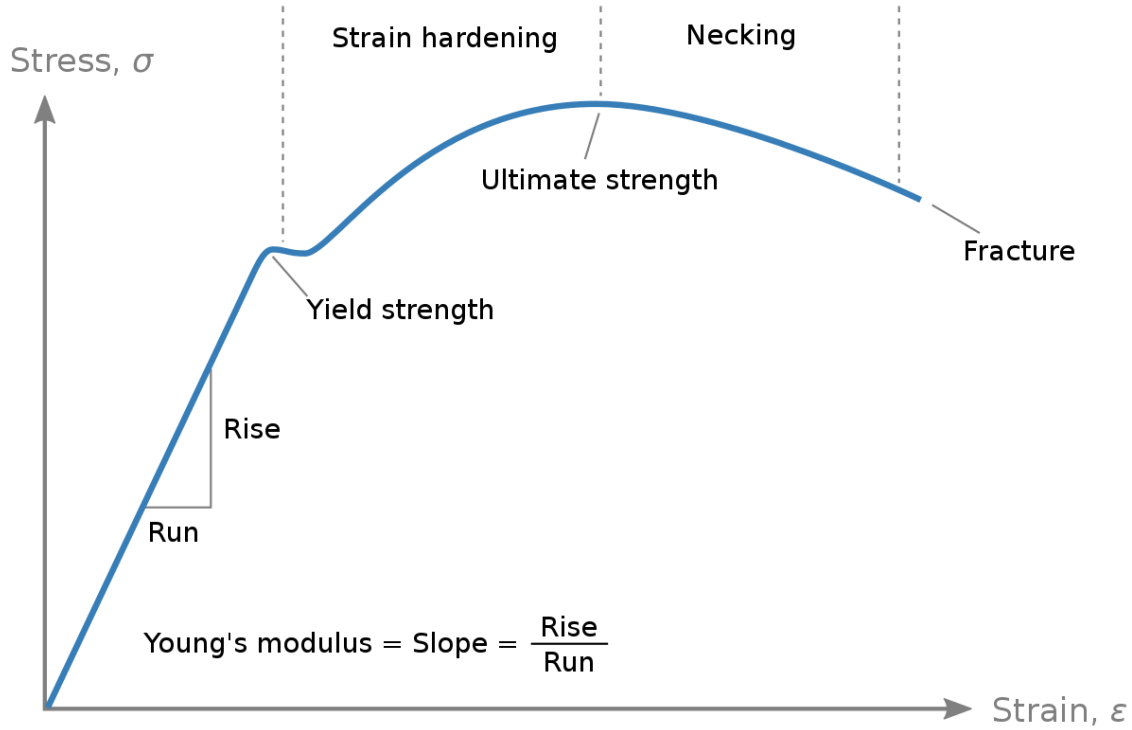

FIGURE 2.2.- Stress-strain graph for ductile material

There is a lot of interesting data to extract from this test. We shall analyze it step by step. For the first part of the test, the specimen will experience elastic deformation, which means that, if the test was to be stopped at any moment during this phase, we would theoretically recover the initial length. The deformation in this stage is given by Hooke´s law which is numerically defined as follows:

$$F = -k.x \qquad (2.1.)$$

Where F is the force, k is the spring constant and x the elongation. Applying this formula to our particular case we find a relationship between the stress, strain and the modulus of elasticity or Young modulus (E):

$$\sigma = E.\varepsilon \qquad (2.2.)$$

After this first phase, having passed the yield strength we now have plastic deformation, the curve shows a counter intuitive shape by going up then going down after the ultimate strength and before the fracture point, the reason for this is the before mentioned voids and porosity of the materials. Before the breaking point, the void growth will require lesser stress. It´s interesting to note that before the ultimate strength the specimen will experiment strain hardening and after it will experiment necking, which is a phenomenon in which the deformation will concentrate in a point. We can see an example of a deformation and fracture in a specimen before and after the experiment in Figure 2.3.

FIGURE 2.3.- Ductile fracture after axial load test

It is worth mentioning that when working with brittle materials it´s difficult to differentiate the elastic from the plastic zone. In this cases, it is assumed that the yield strength is found at 0,2% plastic deformation. As we can see in the following figure:

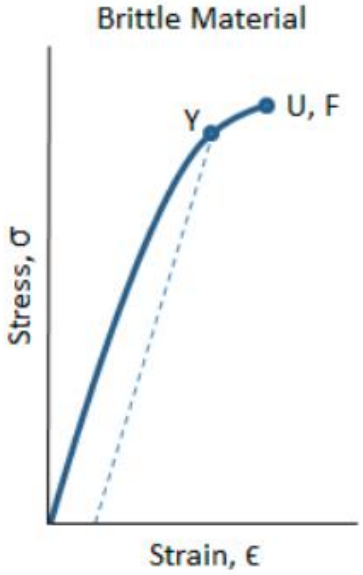

FIGURE 2.4. Axial load test for brittle material

2. 2.- FUNDAMENTALS OF THE FLOW PLASTICITY THEORY

We will now move on to a deeper analysis of the flow plasticity theory. We will understand different concepts that are important for the understanding of plastic flow. During this chapter it´s important to note that the following notation will be used indifferently:

$\Delta\boldsymbol{\sigma_{ij}} \leftrightarrow \Delta\boldsymbol{\varepsilon_{ij}}$ or $\dot{\boldsymbol{\sigma}}_{\boldsymbol{ij}} \leftrightarrow \dot{\boldsymbol{\varepsilon}}_{\boldsymbol{ij}}$ or $\boldsymbol{d\sigma_{ij}} \leftrightarrow \boldsymbol{d\varepsilon_{ij}}$

Flow plasticity theory was developed in the 1930s mainly for metals, but it can also apply to other types of materials. By analyzing a simple traction test on a metal bar we can get a 1D picture (Figure 2.5.) of the plastic deformation.

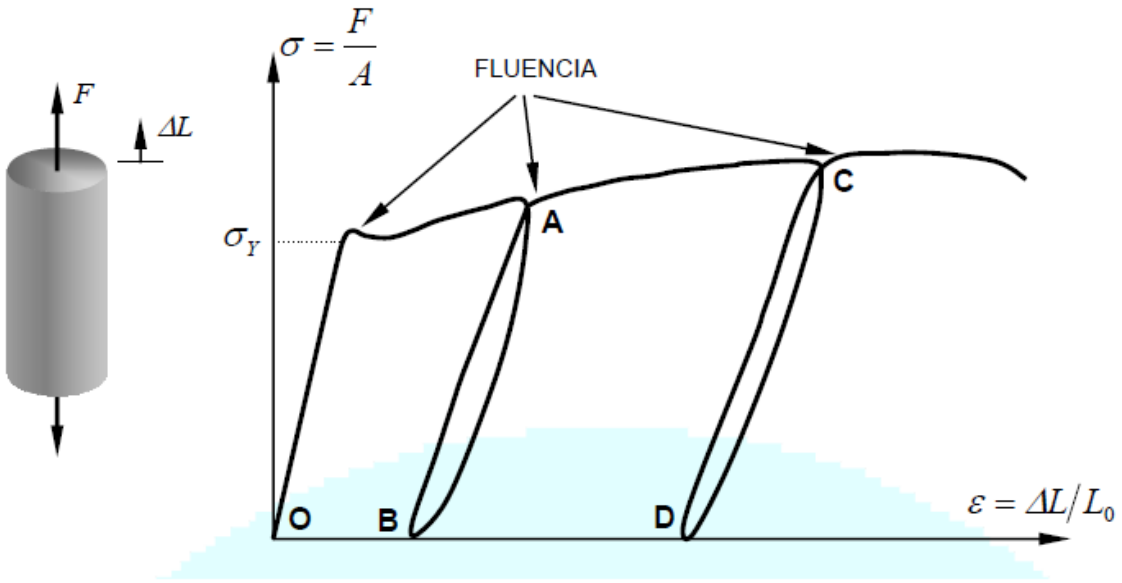

FIGURE 2.5.- Axial load test in which the specimen is loaded and unloaded repeatedly before fracture

We can easily spot a noticeable difference in behavior after reaching the yield stress (σ_Y). After this point a small increase in the tension results in a big deformation, we shall refer to the region after the yield stress as the elasto-plastic region. We can observe that for a deformation OBA we will have elastic (thus recoverable) deformation which will equal the elongation from B to A and plastic deformation which is the elongation from 0 to B.

The previous figure is a good representation of what could be considered an ideal elasto-plastic behavior. Reality is that different materials will behave differently when subjected to this same traction test, as visualized in figure 2.6. In the following figure we can see some oversimplified curves that represent different behaviors:

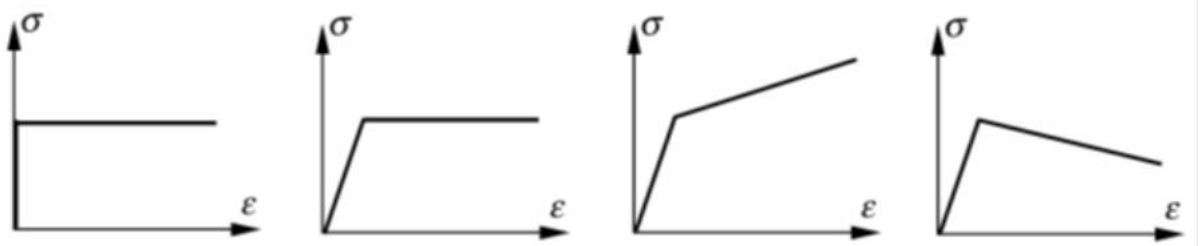

FIGURE 2.6. a) Rigid-perfectly-plastic b) Elastic-perfectly-plastic c) Rigid Linear hardening d) Elastoplastic

2. 2. 1.- Additivity of deformations

As we know from the previous part, when subjected to a tension, a material will experience plastic and elastic deformation. We can apply the principle of additivity to calculate the total deformation, this means that it will be equal to the addition of the elastic deformation plus the plastic deformation:

$$\boldsymbol{d\varepsilon_{ij} = d\varepsilon_{ij}^{e} + d\varepsilon_{ij}^{p}} \qquad (\mathbf{2.3.})$$

In order to calculate the elastic deformation ($\boldsymbol{d\varepsilon_{ij}^{e}}$) we can apply the principles learnt in the previous section about the theory of elasticity:

$$\boldsymbol{d\varepsilon_{ij}^{e} = C_{ijkl} + d\sigma_{kl}} \qquad (\mathbf{2.4.})$$

Where $C = E^{-1}$, and E^{-1} is the inverse of the elastic stiffness matrix. In the following sections we will learn how to calculate the plastic deformation.

2. 2. 2.- Yield surface

The yield surface graphically represents the different combinations of tensions that will result in elastic and plastic deformations (Figure 2.7.). It is of interest as it generalizes the yield limit we had obtained in 1D during the introduction of this chapter.

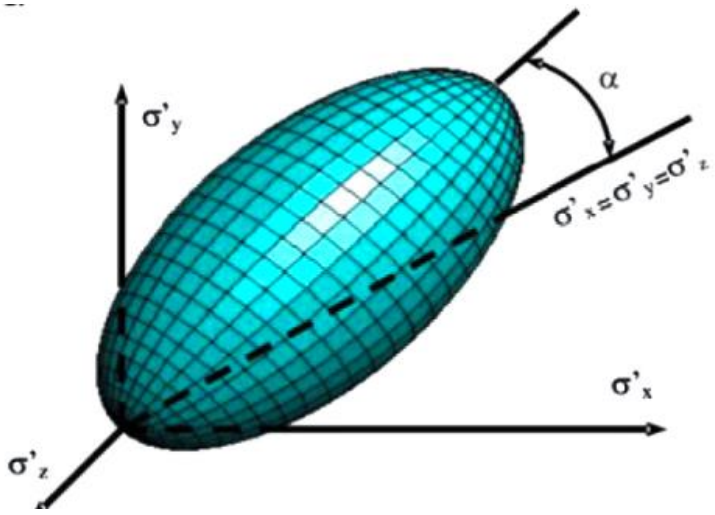

FIGURE 2.7. Yield surface

For the figure above, there will be elastic behavior within the shape and plastic deformations on its surface. The general expression of the yield surface is as follows:

$$F(\sigma_{ij}, \chi_i) = 0 \qquad (2.5.)$$

It is quite intuitive to imagine that for the different elasto-plastic behaviors seen in figure 15 we will have different yield surfaces:

- **Perfect elasto-plastic**: The yield surface is exclusively dependent of the tensions, there will be no shape variation during the load process.
- **Rigid linear hardening**: The yield surface expands during the load process.
- **Elastoplastic**: The yield surface contracts during the load process.

As stated before, the specimen is undergoing plastic deformation when it´s located on the surface of the yield surface. We can make the consideration that:

$$F\left(\sigma_{ij}^{*}, \chi_{ij}^{*}\right) < 0 \;\Rightarrow\; Elastic\ regime$$

$$F\left(\sigma_{ij}^{*}, \chi_{ij}^{*}\right) = 0 \;\Rightarrow\; Elasto\ plastic\ regime$$

$$F\left(\sigma_{ij}^{*}, \chi_{ij}^{*}\right) > 0 \;\Rightarrow\; Impossible$$

2. 2. 3.- Yield law

This law allows us to understand the relationship between the different components of the plastic incremental strain. We shall assume that existence of a function of the stresses:

$$G(\sigma_{ij}, \xi_i) = 0 \qquad (2.6.)$$

This shall be known as elastic potential so that plastic deformations can be calculated as:

$$d\varepsilon_{ij}^{p} = d\lambda \frac{\partial G}{\partial \sigma_{ij}} \qquad (2.7.)$$

Where $d\lambda$ is the numerical value of the plastic deformation, G is the direction of the plastic deformation; the direction of the plastic strain is parallel to the direction of the gradient of the plastic potential.

2. 2. 4.- Hardening law

The hardening expresses the variation in the size, shape, or position of the yield surface. This law does not exist in the case of perfect plasticity, since in this case the yield surface remains constant. Otherwise, if the material is softenable or stiffenable, it is necessary to specify how the yield surface varies and, since the yield surface is defined by expression (2.4.), the hardening law will express the variation of the parameters that appear in that equation. Normally, these parameters are made to depend on the accumulated plastic strain.

$$\boldsymbol{\chi = \chi\left(\varepsilon_{ij}^{p}\right)} \qquad \boldsymbol{(2.8.)}$$

2. 3.- YIELD CRITERION

There are many criterions for the calculation of the point in which plastic deformation starts. Considering the behavior difference between ductile and brittle materials it´s evident that there must be different models for each case. We will now review the most common criterion used nowadays.

2. 3. 1.- Rankine criterion

Rankine criterion should be mostly used for brittle materials and it´s not advisable for ductile ones. The criterion can be defined as:

The yield of the material begins when the maximum normal stress in the material reaches a critical value equal to the yield stress obtained for a specimen of the same material in a uniaxial tensile test.

If we consider the principal stresses to be $\sigma_1 \geq \sigma_2 \geq \sigma_3$, σ_t the failure stress in tension and σ_c the failure stress in compression. The criterion states that there will be failure when:

$$\sigma_1 \geq \sigma_t \quad or \quad \sigma_3 \leq \sigma_c$$

Graphically:

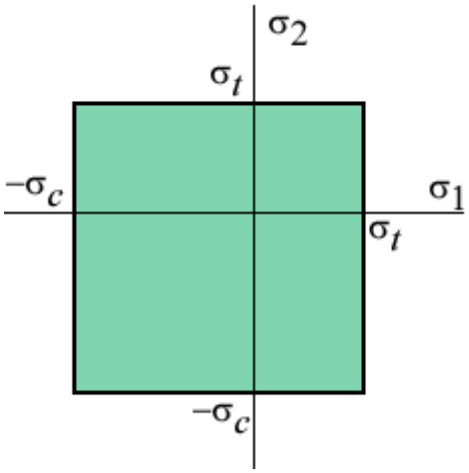

FIGURE 2.8. Graphical representation of the Rankine criterion

2. 3. 2.- Von Mises criterion

Contrary to the Rankine criterion, Von Mises is very useful at analyzing failure criterion on ductile material. It can be defined as:

The von Mises criterion says that when a critical value is reached by the shear energy the yielding of the material will begin. For a general case with three principal stresses:

$$(\sigma_1 - \sigma_2)^2 + (\sigma_2 - \sigma_3)^2 + (\sigma_3 - \sigma_1)^2 = constant$$

The constant is found with the uniaxial test, which means that both σ_2 and σ_3 are zero and σ_1=Y. Then the formula becomes:

$$(\sigma_1 - \sigma_2)^2 + (\sigma_2 - \sigma_3)^2 + (\sigma_3 - \sigma_1)^2 = 2Y^2$$

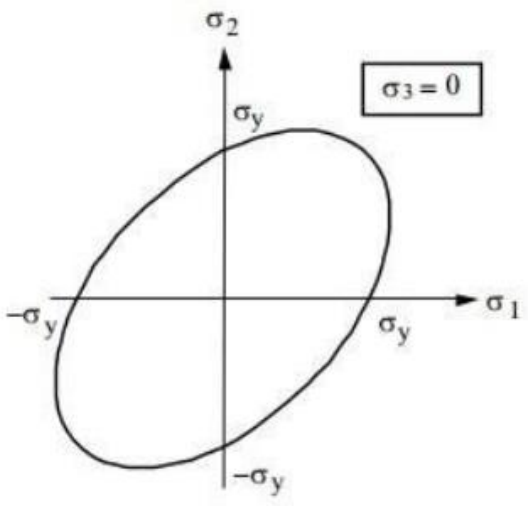

FIGURE 2.9. Graphical representation of the Von Mises criterion

2. 3. 3.- Tresca criterion

Tresca criterion can be considered as an alternative to the Von Mises criterion. It will provide results without as much accuracy as Von Mises but with a higher safety margin. Tresca criterion can be defined as:

The Tresca criterion says that when a critical value is reached by the maximum shear stress (known as shear yield strength) yielding will begin.

If we consider the principal stresses $\sigma_1 \geq \sigma_2 \geq \sigma_3$ we can find the maximum shear stress with the following relationship:

$$\tau_{max} = \frac{1}{2}(\sigma_1 - \sigma_3) \tag{2.9}$$

In a simple axial loading test both σ_2 and σ_3 are zero, then we can find the failure criterion as:

$$\tau_f = \frac{1}{2}\sigma_f \tag{2.10.}$$

Maximum Shear stress for failure can be found just by simply combining both previous equations:

$$\tau_{max} \geq \frac{1}{2}\sigma_f \quad \Leftrightarrow \quad \sigma_1 - \sigma_3 \geq \sigma_f \tag{2.11.}$$

We can graphically observe the difference in the areas produced by the Von Mises and Tresca criterion:

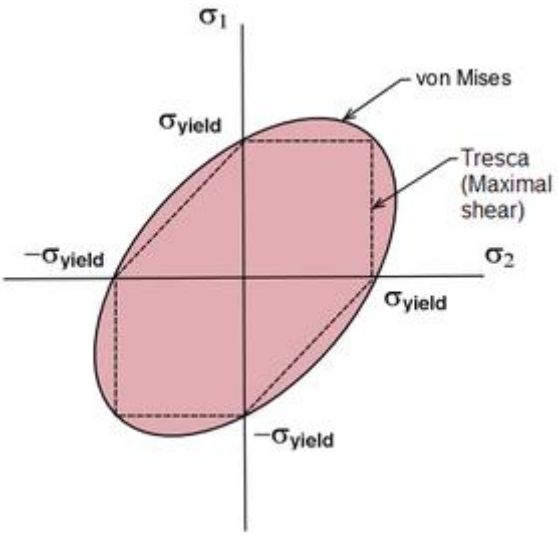

FIGURE 2.10. Comparison between Von Mises and Tresca criterion

2. 3. 4.- Drucker-Prager criterion

The Drucker-Prager criterion is a modification of the Von Mises criterion, a different behavior in traction and compression is considered. In this criterion, an extra hydrostatic-dependant first invariant I_1 and J_2 are introduced to the Von Mises equation:

$$\boldsymbol{f(I_1,J_2) \equiv \alpha I_1 + \sqrt{J_2} - k = 0} \qquad \boldsymbol{(2.12.)}$$

As seen in the equation, there are new material parameters $\boldsymbol{\alpha}$ and k. Both can be calculated as follows:

$$\boldsymbol{\alpha = \frac{2\sin\delta}{\sqrt{3}(3-\sin\delta)}} \qquad \boldsymbol{k = \frac{6c\cos\delta}{\sqrt{3}(3-\sin\delta)}}$$

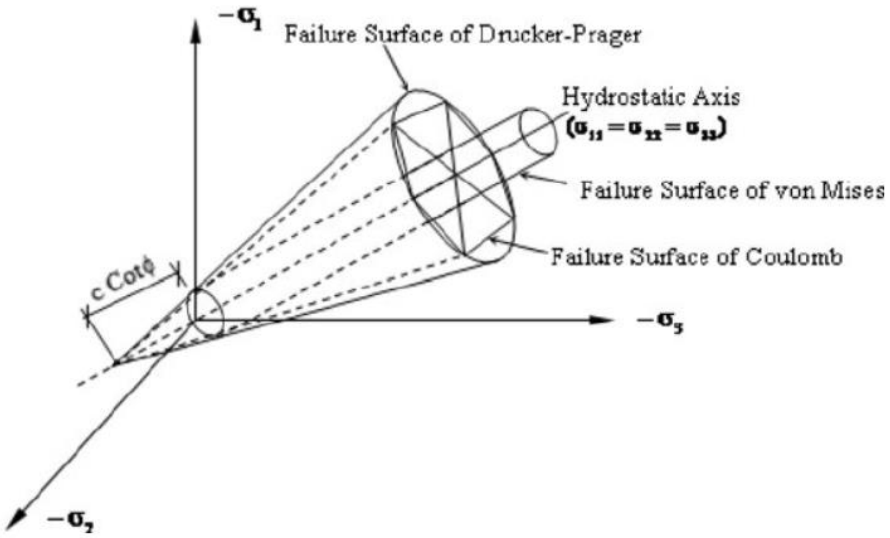

FIGURE 2.11. Graphical representation of the Drucker-Prager criterion

CHAPTER 3

Strain gradient plasticity

Traditionally, when we talked about plastic deformations, we didn´t take into account the different behaviors due to the size of the work piece. Experimental results indicate that the materials show strong size effects when deformed within the plastic zone.

In this chapter we will first study experiments that prove this phenomenon and the dislocations that justify its existence. Then we will move to Gao et al. mechanism-based strain gradient plasticity theory and we will finish by explaining what is an UMAT subroutine for Abaqus and how can we use it to implement the already mentioned mechanism-based strain gradient plasticity theory.

3.1.- INTRODUCTION

There are two simple experiments we can use to clearly see this difference due to size, one is the already mentioned uniaxial loading test and the other one is done by subjecting a cylindrical specimen to a torsion force. The results are as follows:

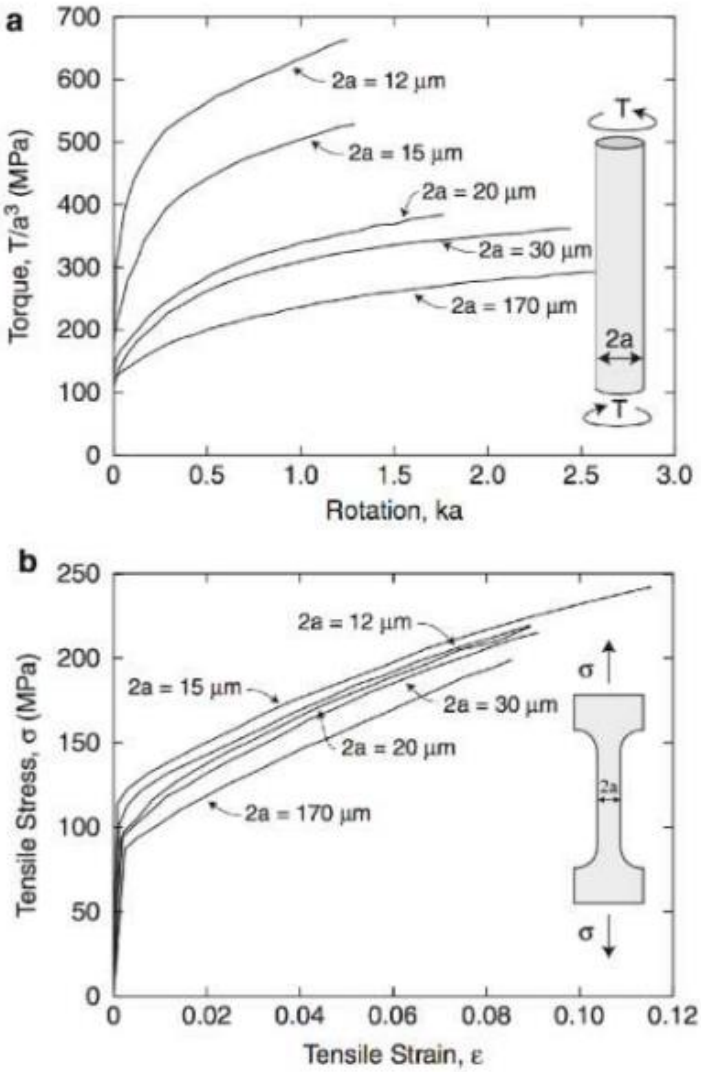

FIGURE 3.1. Experimental tests that show the effect of strain gradient plasticity

As seen in figure 3.1., a reduction of section leads to stronger behavior in both of the test. The reason for this is that the stress at a point may be affected by not only the strain but also the strain gradient if the length scale associated with the deformation field is small, and in this case it becomes necessary to include the strain gradient term in the description of

plasticity deformation at small length scale. We can assume strain gradient to be inverse proportion to the length of the plastic deformation region. A smaller length will mean that a stronger strain gradient effect will be noted

It´s important to understand that when a material is being deformed two kinds of dislocations will appear. On the one hand, there will be statistically stored dislocations (SSDs) and on the other hand there will be geometrically necessary dislocations (GNDs). Statistically stored dislocations accumulate randomly when they trap each other during the deformation process, geometrically necessary dislocations are necessary for compatible deformation of various parts of the material.

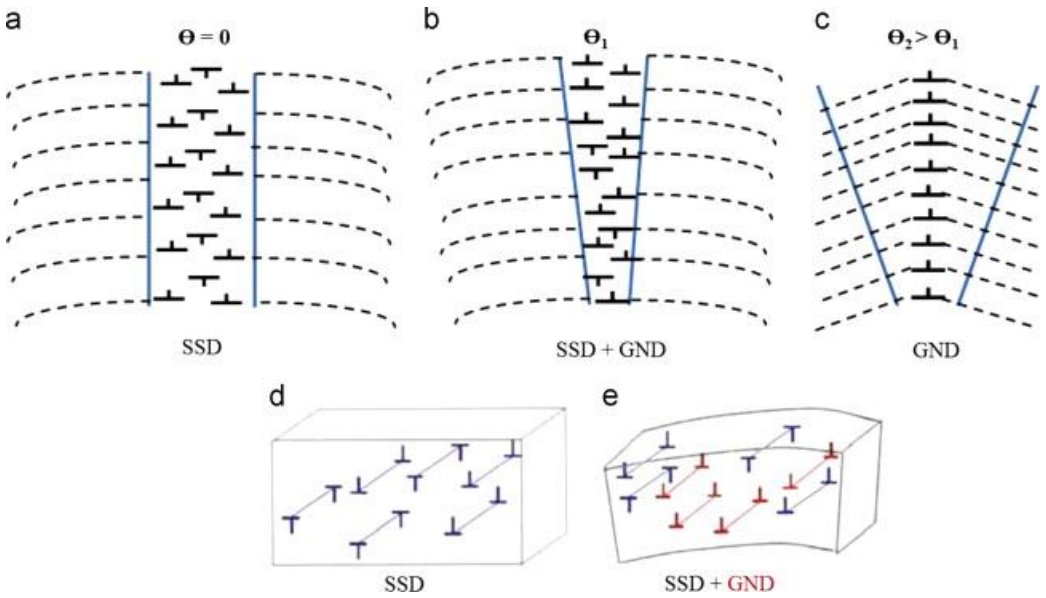

FIGURE 3.2. Illustration of SSD and GND dislocations

When the density of GNDs is bigger than the density of SSDs we can say that GNDs control the work hardening of the material, they do this by becoming “obstacles” to slip. The size effects we saw in figure 3.1. are attributed to GNDs which, in turn, are associated to the plastic strain gradients. Plastic strain gradients appear either because of the geometry of loading or because of the non-uniform deformation of the material.

3. 2.- MECHANISM-BASED STRAIN GRADIENT PLASTICITY THEORY

Gao et al. proposed a mechanism-based strain gradient plasticity theory based on a multiscale framework linking the microscale notion of SSDs and GNDs to the mesoscale notion of plastic strain and strain gradient. This theory assumes that:

1. The motion of the dislocations controls the microscale flow stress, it will happen under the law for strain gradient plasticity, which is as follows:

$$\tilde{\sigma} = \sigma_Y \sqrt{f^2(\tilde{\varepsilon}) + l\eta} \qquad (3.1.)$$

Where $\tilde{\sigma}$ is the stress tensor, $\tilde{\varepsilon}$ is the strain tensor and l is the length of the material:

$$l = 3\alpha^2 \left(\frac{\mu}{\sigma_Y}\right)^2 b$$

Where μ is the shear modulus, b is the Burgers vector and α is an empirical constant which is usually in the range of 0.2 to 0.5.

2. We can define a mesoscale cell as a cell large enough for the application of the Taylor model yet sufficiently small to apply a simplification of the strain field as linear. In this cell, we can assume negligible higher-order strain gradients. The equation that relates the microscale and mesoscale at the mesoscale cell is the plastic work equality:

$$\int_{Vcell} \tilde{\sigma}'_{ij} \delta\tilde{\varepsilon}_{ij} dV = \left(\sigma'_{ij} \delta\varepsilon_{ij} + \tau'_{ijk} \delta\eta_{ijk}\right) Vcell \qquad (3.3.)$$

Where σ is the tension, ε is the strain, τ is the higher-order stress and η is the strain gradient.

3. The fundamentals of the conventional theory of plasticity are preserved when working on a microscale. We shall assume that the Schmid stress is proportional to the dislocation slip so we can obtain the following relationship:

$$\frac{d\tilde{\varepsilon}_{ij}}{d\tilde{\varepsilon}} = \frac{3\tilde{\sigma}'_{ij}}{2\tilde{\sigma}_e} \qquad (3.4.)$$

Where $d\tilde{\varepsilon}_{ij}$ is the effective strain increment and $\tilde{\sigma}_e$ is the effective stress. We can obtain their values through the following formulas:

$$d\tilde{\varepsilon} = \sqrt{\frac{2}{3} d\tilde{\varepsilon}_{ij} d\tilde{\varepsilon}_{ij}} \qquad (3.5.)$$

$$\tilde{\sigma}_e = \sqrt{\frac{2}{3} \tilde{\sigma}'_{ij} \tilde{\sigma}'_{ij}} \qquad (3.6.)$$

The microscale yield criterion is $\tilde{\sigma}_e = \tilde{\sigma}$ and the effective strain can be calculated:

$$\tilde{\varepsilon}^2 = \frac{2}{3} \tilde{\varepsilon}_{ij} \tilde{\varepsilon}_{ij} \qquad (3.7.)$$

$$\tilde{\varepsilon} \delta \tilde{\varepsilon} = \frac{2}{3} \tilde{\varepsilon}_{ij} \delta \tilde{\varepsilon}_{ij} \qquad (3.8.)$$

These three assumptions are of crucial important when trying to analyze and understand the mechanism-based strain gradient plasticity theory. We shall now consider a cubic unit cell in mesoscale whose edges are all l_ε, a value much shorter than the l calculated before. We can then find the following relationship for the microscale strain, strain gradient and mesoscale strain:

$$\tilde{\varepsilon}_{ij} = \varepsilon_{ij} + \frac{1}{2}(\eta_{kij} + \eta_{kji})x_k \qquad (3.9.)$$

In which x_k represents the local coordinates with origins at the center of the cell. If we substitute the following kinematic assumption into the equation:

$$\delta\tilde{\varepsilon}_{ij} = \delta\varepsilon_{ij} + \frac{1}{2}(\delta\eta_{kij} + \delta\eta_{kji})x_k \qquad (3.10)$$

And assuming σ'_{ij} and τ'_{ijk} can be represented by the following equations:

$$\sigma'_{ij} = \frac{1}{V_{cell}}\int_{V_{cell}} \tilde{\sigma}'_{ij} dV \qquad (3.11.)$$

$$\tau'_{ijk} = \frac{1}{V_{cell}} Dev\left[\frac{1}{2}\int_{V_{cell}} \tilde{\sigma}'_{jk}\, x_i + \tilde{\sigma}'_{ik} x_j dV\right] \qquad (3.12.)$$

Where Dev [...] represents the deviatoric part of […]. Given x_k is located at the center of the cell, we can make the following assumptions that will help us solve the integral above:

$$\frac{1}{V_{cell}}\int_{V_{cell}} dV = 1, \qquad \int_{V_{cell}} x_k\, dV = 0, \qquad \frac{1}{V_{cell}}\int_{V_{cell}} x_k x_m dV = \frac{1}{12} l_\varepsilon^2 \delta_{km}$$

Then the equations that represent the mechanism-based strain gradient can finally be simplified as:

$$\sigma'_{ij} = \frac{2\varepsilon_{ij}}{3\varepsilon}\sigma \qquad (3.13.)$$

$$\boldsymbol{\tau'_{ijk} = l_{\varepsilon}^{2}\left[\frac{\sigma}{\varepsilon}\left(\Lambda_{ijk} - \Pi_{ijk}\right) + \frac{\sigma_{Y}^{2} f(\varepsilon) f'(\varepsilon)}{\sigma}\Pi_{ijk}\right]} \qquad (3.14)$$

Where Λ_{ijk} and Π_{ijk} are:

$$\boldsymbol{\Lambda_{ijk} = \frac{1}{72}\left[2\eta_{ijk} + \eta_{kji} + \eta_{kij} - \frac{1}{4}\left(\delta_{ik}\eta_{ppj} + \delta_{jk}\eta_{ppi}\right)\right]} \qquad (3.15)$$

$$\boldsymbol{\Pi_{ijk} = \frac{1}{54}\frac{\varepsilon_{mn}}{\varepsilon^{2}}\left[\varepsilon_{ik}\eta_{jmn} + \varepsilon_{jk}\eta_{imn} - \frac{1}{4}\left(\delta_{ik}\varepsilon_{jp} + \delta_{jk}\varepsilon_{ip}\right)\eta_{pmn}\right]} \qquad (3.16)$$

The flow stress is then:

$$\boldsymbol{\sigma = \sigma_{Y}\sqrt{f^{2}(\varepsilon) + l\eta}} \qquad (3.17)$$

It´s easy to imagine the importance of the chosen value for l_{ε} as it controls the accuracy of the strain gradient calculation, it should be small enough to guarantee the accuracy but large enough to contain enough dislocations for obtaining accuracy on the flow stress calculation. Gao combined these two requirements and gave result to the following equation:

$$\boldsymbol{l_{\varepsilon} = \beta L_{yield} = \beta\frac{\mu b}{\sigma_{Y}}} \qquad (3.18.)$$

In this equation, $\boldsymbol{L_{yield}}$ is the mean spacing between SSDs at plastic yielding and $\boldsymbol{\beta}$ is a constant to be determined through empirical means. In order to guarantee a representative sample of dislocations the value of $\boldsymbol{\beta}$ should be bigger than one.

3. 3.- UMAT SUBROUTINE

UMAT stands for user material. An UMAT subroutine allows us to confer special mechanical properties to the material being analyzed. In order to understand what is an UMAT, it is important to take into account how ABAQUS solves the FEM models. Assuming that we deal with single “step” models, we can understand a “step” as a load case, which will have both boundary conditions and loads associated to every one of them. However, we can make a new "step" to obtain the modified characteristics of the model, for example let's suppose that we are dealing with a model with an elasto-plastic behavior and we subject the model to a "step" that produces the plastification of a certain area of the model, we could create a step that would follow the previous one so that the new “step” would consider that area of the model to have experienced the plastic deformation.

The "step" is assigned a time, which has physical meaning if we are in a dynamic case, but not interesting for our case. The steps consist of a series of increments, and at each increment an “increment” of the applied loads is applied. In each increment, a series of iterations will be carried out to reach equilibrium with the loads corresponding to this increment. In the event that the maximum number of allowed iterations has been used and the problem does not converge, the solution that did not reach equilibrium is discarded and a new increment is performed with a load step smaller than the one previously given.

In Figure 3.3. we can see a diagram of the process that ABAQUS follows to solve problems, and where it calls the UMAT subroutine. Although the indicated scheme can show in a simple way how ABAQUS works and where the UMAT subroutine is executed, it is not valid for the first iteration of any element. In this first iteration the UMAT subroutine is called twice, in the first call the stiffness matrix is assembled using the configuration of the initial situation in the increment. The second call updates the stiffness based on the updated setting from the previous iteration. In the other iterations the initial configuration will be based on the previous iteration. In each iteration that is carried out to search for equilibrium and for each integration point of each element, the UMAT subroutine is executed.

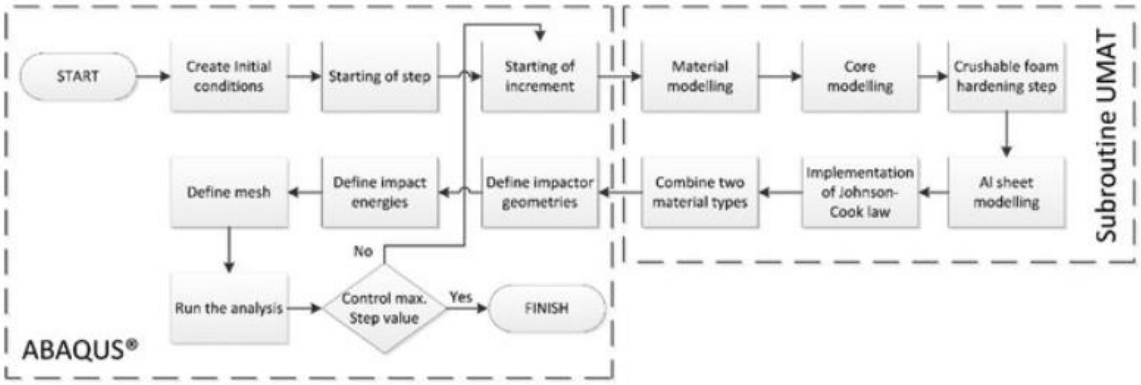

FIGURE 3.3.- Flowchart of Abaqus and the UMAT subroutine

For each iteration, ABAQUS passes to the subroutine the stresses and strains at the beginning of the iteration and the predicted increase in strains. From the data that we have introduced to the subroutine, it will then return to ABAQUS the Jacobian matrix and the updated tensions.

3. 3. 1.- Variables

The following is a list of the most common variables used in an Abaqus subroutine. They will play a crucial role on defining the material properties:

- **DDSDDE (NTENS, NTENS):** Jacobian matrix of the material model. Because for our model we will assume small deformations of the interface the Jacobian matrix will be expressed as $C = \partial\Delta\sigma/\partial\Delta\varepsilon$ in which $\Delta\sigma$ is the increments in tensions and $\Delta\varepsilon$ is the increment in deformations. The components of matrix DDSDDE (I, J) are understood as the changes the i-th stress experiences at the end of each of the increment, caused by an infinitesimal perturbation in the j-th component of the strain vector. In ABAQUS/Standard, only the symmetric part of DDSDDE, unless solving non-symmetric equations is enabled for the defined material.

- **STRESS (NTENS):** It is a vector which contains the stress tensor in reduced Voight notation at the beginning of the subroutine, and has to be updated in the subroutine to be the stress tensor at the end of each iteration. The direction of the stresses will take the element local directions.

- **STATEV (NSTATEV):** It is a vector where we can store a variable that depends on the solution of the state variables (stress and strain). There is one STATEV variable for each integration point in the model, and the value at the beginning of an iteration is the value of the previous increment, unless changed by one of the USDFLD or UEXPAN subroutines. The size of this vector is defined using the DEVPAR command (in the inp file when calling the material). Also keep in mind that the STATEV variables will be shown in the output file (odb) with the name of SDVs (solution-dependnt variables).

I will now proceed to mention another, less relevant, variables just for the information of the reader:

- **STRAN (NTENS):** Similar to STRESS, a vector which will contain the strain tensor in reduced Voigh total notation but in this case at the beginning of each increment. These deformations will take the local direction of the element.

- **DSTRAN (NTENS)**: The variations of the deformations are contained in this vector. This increase in deformations will also take the local direction of the element.

- **NTENS**: It indicates the number of components included in the Tension pseudovector, depending on the type of element used. For plane stress elements the number of components is 3, in the case of plane strain it is 4 and for the three-dimensional case it is 6.

- **NSTATEV**: Reflects the number of dependent variables in the solution variables

- **NOEL**: It´s as simple as the element number
- **NPT**: Refers to the Integration Point Number
- **KSTEP**: Step number
- **KINC**: Increment number

3. 3. 2.- Format

As we must know, an UMAT subroutine is written in Fortran. Every subroutine will be different, but there is a common format that will be found at the beginning of every one of them which can be seen in figure 3.4.

```
SUBROUTINE UMAT(STRESS, STATEV, DDSDDE, SSE, SPD, SCD,
     1  RPL, DDSDDT, DRPLDE, DRPLDT,
     2  STRAN, DSTRAN, TIME, DTIME, TEMP, DTEMP, PREDEF, DPRED, CMNAME,
     3  NDI, NSHR, NTENS, NSTATV, PROPS, NPROPS, COORDS, DROT, PNEWDT,
     4  CELENT,DFGRDO,DFGRD1,NOEL,NPT,LAYER,LSPT,LSTEP,LINC)

       INCLUDE 'ABA_PARAM.INC'
        CHARACTER*8 CMNAME

DIMENSION STRESS(NTENS), STATEV(NSTATV),
     1  DDSDDE(NTENS,NTENS),
     2  DDSDDT(NTENS), DRPLDE(NTENS),
     3  STRAN(NTENS), DSTRAN(NTENS), TIME(2), PREDEF(1), DPRED(1),
     4  PROPS(NPROPS), COORDS(3), DROT(3,3),DFGRD0(3,3),DFGRD1(3,3)
```

FIGURE 3.4. Format of Abaqus UMAT subroutine

3. 3. 3.- Mechanism-based strain gradient plasticity implementation in Abaqus

In section 3. 1. It was explained what the mechanism-based SGP proposed by Gao et al. consists of, this mechanism is useful for simple calculations like pure bending, but when we turn our focus in more complex calculations we will need to use numerical methods. This is when Abaqus and subroutines come into play.

As function of their order we can differentiate two different types of SGP theories: the first one including higher order stresses thus requiring extra boundary conditions, and a second one which will not include higher order terms, gradient effects are then considered through the incremental plastic moduli. It´s of our interest the use of the CMSG plasticity theory developed by Huang et al., which relies on Taylor´s dislocation model (which will be explained in the next section) as it will not include higher order. The plastic strain gradient will only appear in the constitutive model while both the equilibrium equations and the boundary conditions are the same as the conventional continuum theories.

3. 3. 3. 1.- A Taylor-based viscoplastic-like constitutive relation

The Taylor dislocation model proposed by Qu 2004 gives the flow stress depending on both the equivalent plastic strain ε^p and the effective plastic strain gradient η^p:

$$\dot{\boldsymbol{\sigma}} = \frac{\partial \boldsymbol{\sigma}}{\partial \boldsymbol{\varepsilon^p}} \dot{\boldsymbol{\varepsilon}}^{\boldsymbol{p}} + \frac{\partial \boldsymbol{\sigma}}{\partial \eta^{\boldsymbol{p}}} \dot{\eta}^{\boldsymbol{p}} \qquad (3.19.)$$

The problem when using this model is that for plastic strain rate ε_{ij}^p proportional to the deviatoric stress σ_{ij}', we can´t obtain a self cointained constitutive model because of $\dot{\eta}^{\boldsymbol{p}}$. Huang et al. proposed a viscoplastic formulation that will give $\dot{\varepsilon}^p$ in terms of effective stress σ_e instead of its rate $\dot{\sigma}_e$:

$$\dot{\varepsilon}^p = \dot{\varepsilon} \left[\frac{\sigma_e}{\sigma_{flow}} \right]^m \qquad (3.20.)$$

Because we are interested in making a model independent of time, Huang et al. prove that for big values for m ($m \geq 20$) we can assume our model to be independent. This means that the velocity of deformation will not influence the results. If we take into account that

the volumetric strain rate ($\dot{\varepsilon}_{kk}$) and the deviatoric strain rate ($\dot{\varepsilon}'_{kk}$) are related to the stress rate in the same way as classical plasticity, the constitutive equation is:

$$\dot{\sigma}_{ij} = K\dot{\varepsilon}_{kk}\delta_{ij} + 2\mu\left\{\dot{\varepsilon}'_{ij} - \frac{3\dot{\varepsilon}}{2\sigma_e}\left[\frac{\sigma_e}{\sigma_{flow}}\right]^m \dot{\sigma}'_{ij}\right\} \tag{3.21}$$

For which:

$$\sigma_{flow} = \sigma_{ref}\sqrt{f^2(\varepsilon^p) + l\eta^p} \tag{3.22.}$$

For these two equations we can find that K is the bulk modulus, μ is the shear modulus, δ_{ij} is the Kronecker delta, σ_{ref} a reference stress, $f^2(\varepsilon^p)$ a non-dimensional function determined from the uniaxial stress-strain curve, l the intrinsic material length, $\dot{\varepsilon}'_{ij}$ the total strain and $\dot{\sigma}_{ij}$ the Cauchy stress tensor.

3. 3. 3. 2.- Consistent tangent modulus

Given we are not taking into account higher order stresses, the equations for CMSG plasticity are pretty much the same as in traditional plasticity. For this reason, the plastic strain rate $\dot{\varepsilon}^p_{ij}$ is proportional to the deviatoric stress rate σ'_{ij}:

$$\dot{\varepsilon}^p_{ij} = \frac{3\dot{\varepsilon}^p}{2\sigma_e}\sigma'_{ij} \tag{3.23.}$$

Where the deviatoric stresses can be found from the following equation in which $|_t$ stands for the value at the beginning of the increment and Δ refers to the incremental value:

$$\sigma'_{ij} = 2\mu\left(\varepsilon'^e_{ij}|_t + \Delta\varepsilon'_{ij} - \Delta\varepsilon^p_{ij}\right) \tag{3.24}$$

The effective stress and the equivalent strain rate can be expressed as simple as:

$$\sigma_e = \sqrt{\frac{3}{2}\sigma'_{ij}\sigma'_{ij}} \tag{3.25}$$

$$\dot{\varepsilon} = \sqrt{\frac{2}{3}\varepsilon'_{ij}\varepsilon'_{ij}} \tag{3.26}$$

Now, by substitution of equation (3.23.) into equation (3.24) we get:

$$\sigma'_{ij} = 2\mu \left(\varepsilon'^{e}_{ij}|_t + \Delta\varepsilon'_{ij} - \frac{3\Delta\varepsilon^p}{2\sigma_e}\sigma'_{ij}\right) \tag{3.27}$$

If we define $\varepsilon'^{e}_{ij}|_t + \ +\Delta\varepsilon'_{ij} = \ \hat{\varepsilon}'_{ij}$ then:

$$\left(1 + \frac{3\mu}{\sigma_e}\Delta\varepsilon^p\right)\sigma'_{ij} = 2\mu\ \hat{\varepsilon}'_{ij} \tag{3.28}$$

Taking the inner part:

$$\sigma_e + 3\mu\Delta\varepsilon^p = 3\mu\hat{\varepsilon} \tag{3.29}$$

Where $\hat{\varepsilon} = \sqrt{\frac{2}{3}\hat{\varepsilon}'_{ij}\hat{\varepsilon}'_{ij}}$ reformulating (3.29.) and substituting (3.20.) and (3.22.):

$$\sigma_e - 3\mu(\hat{\varepsilon} - \Delta\varepsilon\left(\frac{\sigma_e}{\sigma_{flow}}\right)^m) = 0$$

This is a non-linear equation that can be solved with the Newton-Raphson method:

$$\sigma_e = \sigma_e + \frac{3\mu(\hat{\varepsilon} - \Delta\varepsilon\left(\frac{\sigma_e}{\sigma_{flow}}\right)^m) - \sigma_e}{1 + 3\mu h} \tag{3.31}$$

For which h is:

$$h = m\Delta\varepsilon(\frac{\sigma_e}{\sigma_{flow}})^{(m-1)}\frac{1}{\sigma_{flow}}$$

Once the convergence has been achieved we will obtain the incremental effective plastic strain from:

$$\Delta\varepsilon^p = \hat{\varepsilon} - \frac{\sigma_e}{3\mu} \tag{3.33.}$$

From the previous equations we can obtain the value for σ'_{ij} and $\Delta\varepsilon^p_{ij}$. The consistent material Jacobian is computed from equation (3.28.) with respect to all quantities at the end of an increment:

$$\left(1 + \frac{3\mu}{\sigma_e}\Delta\varepsilon^p\right)\partial\sigma'_{ij} + \sigma'_{ij}\frac{3\mu}{\sigma_e}\left(\partial\Delta\varepsilon^p - \frac{\Delta\varepsilon^p}{\sigma_e}\partial\sigma_e\right) = 2\mu\partial\hat{\varepsilon}'_{ij} \tag{3.34}$$

Equation (3.29.) gives to:

$$\partial\sigma_e + 3\mu\partial\Delta\varepsilon^p = 3\mu\partial\hat{\varepsilon} \tag{3.35}$$

By substitution and rearrangement in equation (3.33.):

$$\partial\sigma_e = \frac{3\mu}{1+3\mu h}\partial\hat{\varepsilon} \tag{3.36}$$

By the definition of $\hat{\varepsilon}$ we will get:

$$\partial\sigma_e = \frac{2}{3\hat{\varepsilon}}\frac{3\mu}{1+3\mu h}\hat{\varepsilon}'_{ij}\partial\hat{\varepsilon}'_{ij} \tag{3.37}$$

Substituting this in equation (3.34.) we finally get:

$$\partial\sigma'_{ij} = \left(\frac{2\sigma_e}{3\hat{\varepsilon}}I_{ijkl} - \frac{1}{\sigma_e\hat{\varepsilon}}\left(h - \frac{\Delta\varepsilon^p}{\sigma_e}\right)\frac{3\mu}{1+3\mu h}\sigma'_{ij}\sigma'_{ij}\right)\partial\hat{\varepsilon}'_{ij} \tag{3.38}$$

I_{ijkl} is the fourth-order unit tensor. Finally, considering the before mentioned relationships between stress and strain tensors with deviatoric quantities, the material stiffness matrix is:

$$\partial\sigma_{ij} = \left(\frac{2\sigma_e}{3\hat{\varepsilon}}I_{ijkl} + \left(K - \frac{2\sigma_e}{9\hat{\varepsilon}}\right)I_{ij} - \frac{1}{\sigma_e\hat{\varepsilon}}\left(h - \frac{\Delta\varepsilon^p}{\sigma_e}\right)\frac{3\mu}{1+3\mu h}\sigma'_{ij}\sigma'_{ij}\right)\partial\varepsilon_{ij} \tag{3.39}$$

CHAPTER 4

Abaqus model

In this chapter we will proceed to develop the Abaqus model that will be used to obtain the results of this study, developing an accurate model can sometimes be difficult but the accuracy needs to be high if we want to trust the results obtained. Secondly, we will study the properties of a material used for the labs experiments we will use as reference in order to introduce it to the model.

Having developed the model and found the properties of the material, we will run abaqus with the subroutine to obtain results that we hope will prove the existence of the already known strain gradient plasticity. We will also compare these results to the lab experiments in order to evaluate the degree of accuracy of the results.

4. 1.- EXPERIMENTAL ASSEMBLY

We will reproduce in Abaqus a model to recreate the fracture process in a Small Punch Test (SPT). The SPT is a reliable test that allows us to get accurate data on damage properties and fracture estimation for a specimen, its interest in industry is that, while it allows us to get the mentioned accuracy, it requires a very small testing specimen, which may be required for certain materials.

In a SPT, a very small circular specimen (typical dimensions: 3-8 mm of diameter and 0,25-0,5 mm of thickness) is pressed between two dies that will hold it in place, then, a punch with hemispherical indenter will penetrate the specimen at a speed of v=0,2 mm/min. The results of this experiment are measured by the experimental device that will register the displacement and force required along the experimental process. The following figure represents a standard SPT and it will be the one that will be used as reference for our Abaqus model:

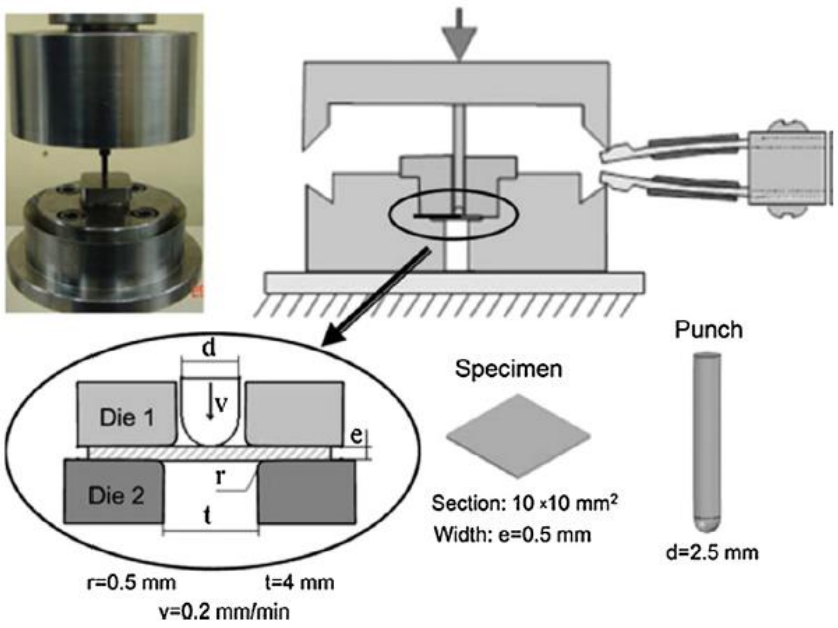

FIGURE 4.1. Device and schematic of the SPT

When translating this model into Abaqus we will preserve the same size characteristics of the specimen and punch. It´s interesting to use axisymmetric for the design of the assembly, it will allow us to obtain the same results but with a much faster analysis.

In the image below it can be seen the Abaqus representation of the experiment in figure 4.2. taking into account the already mention axisymmetric nature of the model:

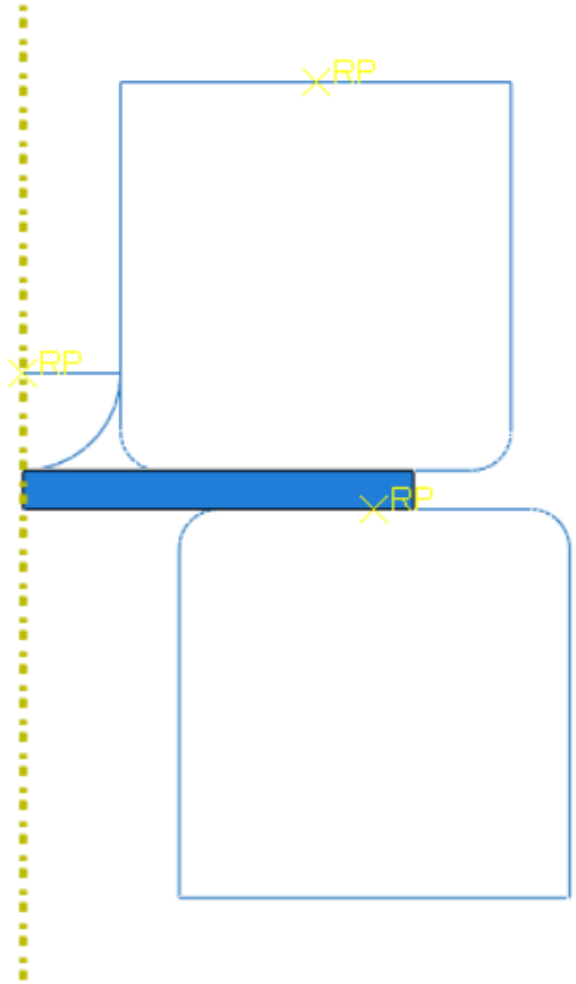

FIGURE 4.2. Model of SPT done in Abaqus

On a first sight the reader will notice the different aspect of the dies and the punch compared to the specimen, this is because they are designed as analytical rigid parts, which means that they are rigid parts in the contact analysis. Given we consider these parts as rigid

and undeformable, describing them as analytical rigid is computationally less expensive as no mesh is needed.

4. 2.- MESH

The mesh may well be the most characteristic element in a finite element analysis, it describes an array of finite elements that will be considered for the calculations. When we mesh a geometry we are discretizing its shape.

For the specimen in the SPT we need to develop a mesh, for it we must find a balance between performance and computational load and the accuracy of results. A finer mesh gives higher accuracy of calculation but the increment in the number of elements increases the time of calculation. This is how our specimen mesh looks like:

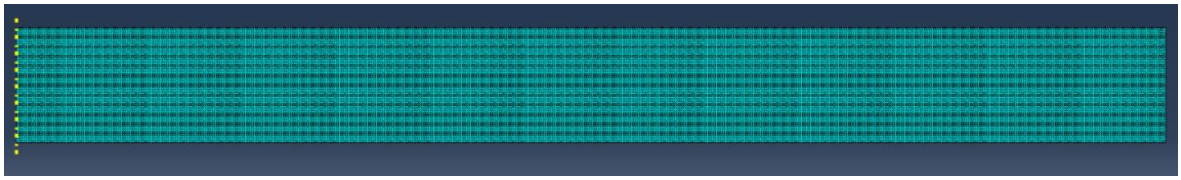

FIGURE 4.3. Meshed specimen for SPT

The later image may be confusion inducing as no clear geometry can be seen in the shape from this distance. If we take a much closer look we can get a general idea of the whole geometry of the work piece:

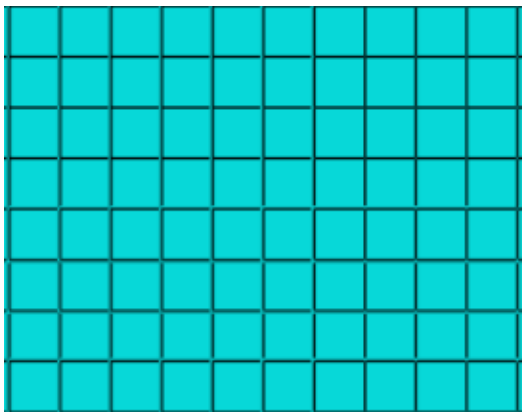

FIGURE 4.4.- Closer look at the mesh

Seeing from this distance, we can appreciate that the mesh displays a quadrilateral shape which is perfect for the rectangular geometry of our specimen. In terms of the mesh type I have used CAX4 which is a 4-node bilinear axisymmetric quadrilateral, hourglass control. The element type of the mesh determines the mathematical algorithms that the software will use when determining the behavior of the model during the simulation stage.

4. 3.- BOUNDARY CONDITIONS

Boundary conditions set the rules of what happens during the simulation process. They are crucial as they will completely define the behavior of the whole model. For our case we will have different boundary conditions that will fix the degrees of freedom of the different elements of the model and also an extra boundary condition that will define the movement speed of the punch.

Having set the reference points for the dies and the punch (seen in figure 4.2.) we can apply a set a boundary conditions on them to define their DoF. Given they are rigid bodies the conditions applied to each of the reference points will apply to all of the part.

For the dies we will have a complete encastre, that way they will not move or rotate in any axis. For the punch we will have conditions that will impede rotation and allow movement on the Y axis, besides this it will experience a BC that will force it to move downwards on the Y axis with the speed of 0,2 mm/min

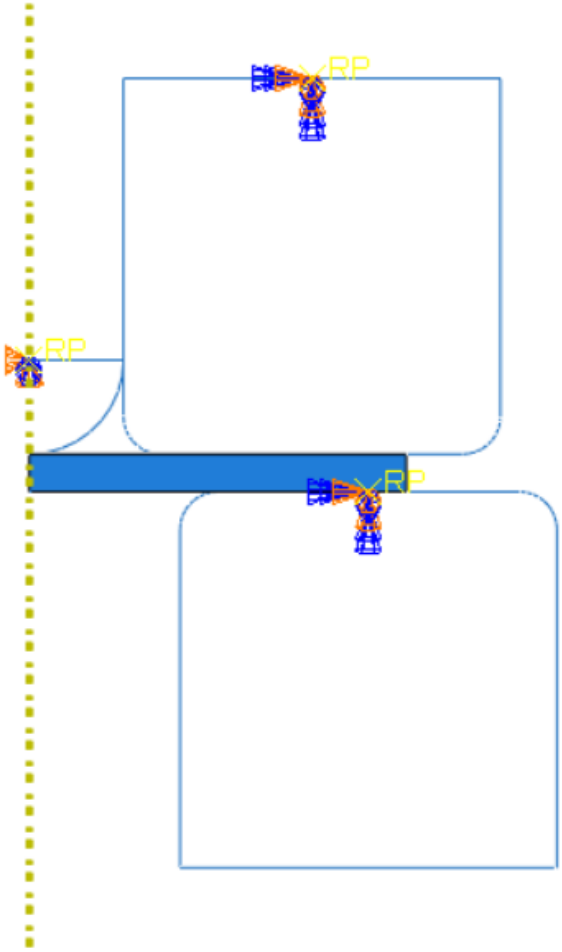

FIGURE 4.5.- Abaqus SPT model with boundary conditions

4. 4.- MATERIAL PROPERTIES

The first step on this process was to determine the properties of a material used for several experiments conducted in the lab, the reason for this is that we want to compare our model to the lab results in order to evaluate the accuracy of it. The following graphs represent the results of such lab experiments, for all of them, the same material is used and the thickness is reduced from 500 μm to a minimum of 40 μm.

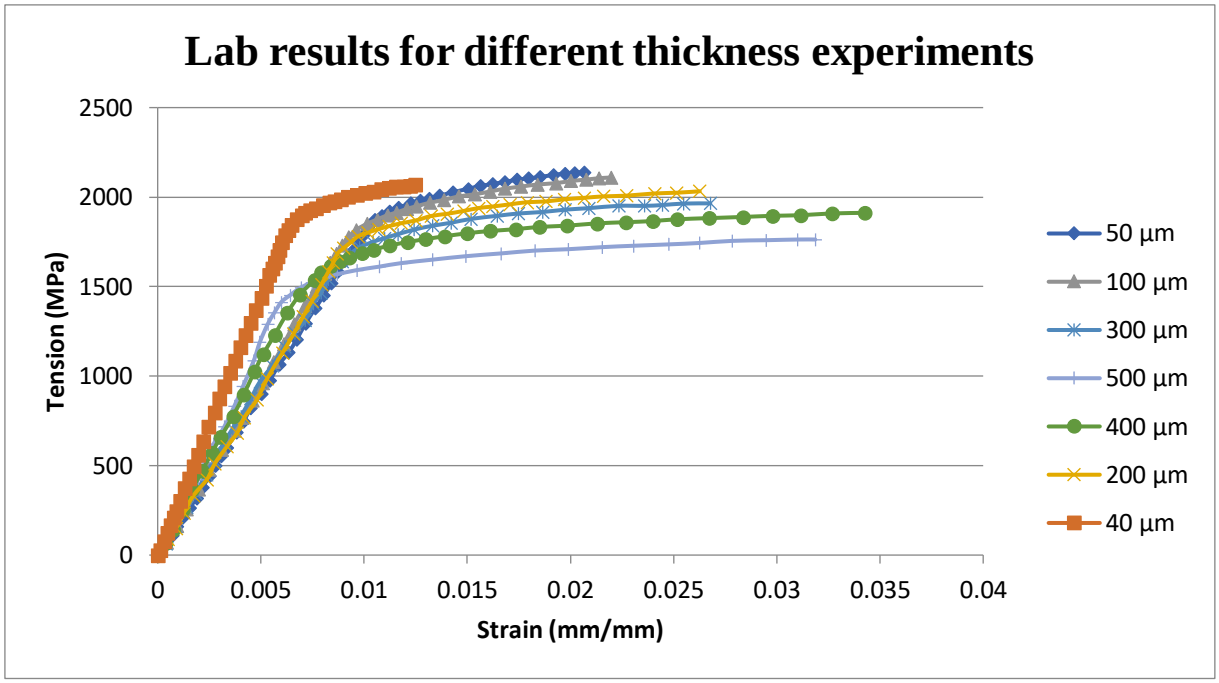

FIGURE 4.6.- Lab results for tension-strain relationship at different thickness

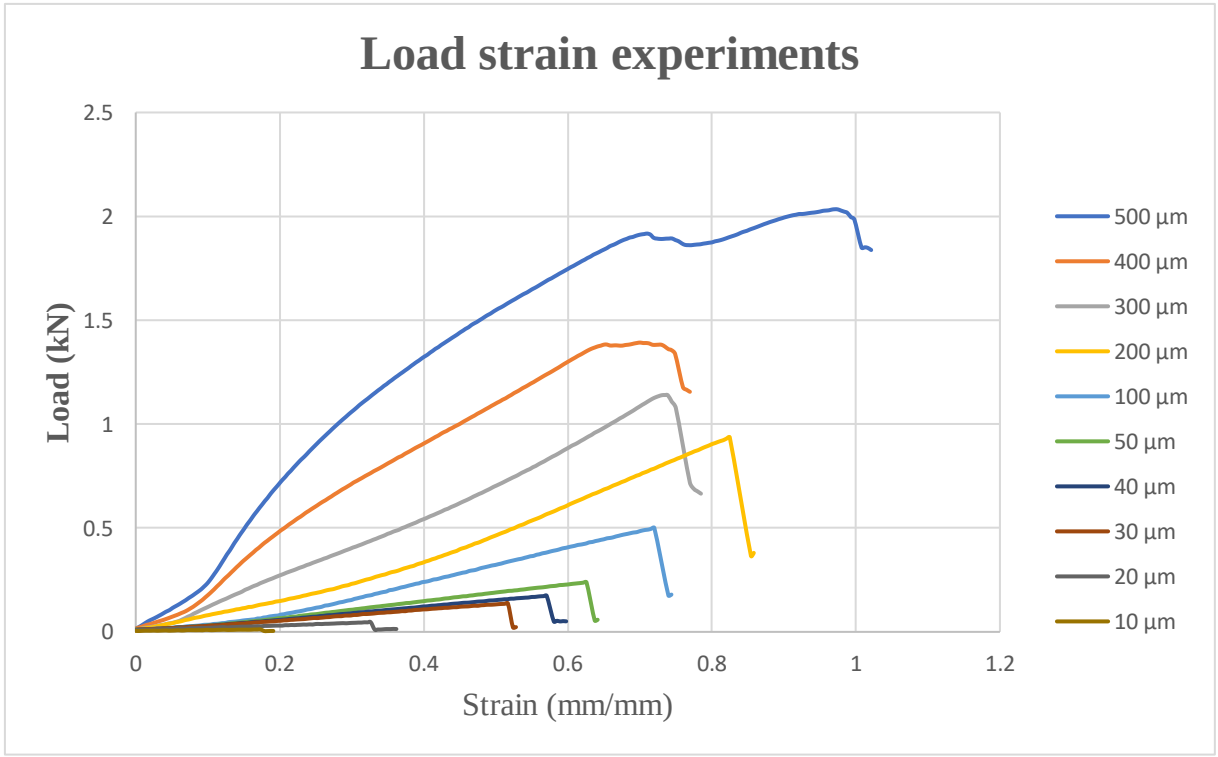

FIGURE 4.7.- Lab results for load-strain relationship at different thickness

In the first graph we see several plots comparing the behaviors at different thickness in a stress-strain graph, for the second one we see the behaviors for a load-strain graph. The reader might have noticed something, even if intuition correctly leads us to believe that thicker specimens will record higher loads before fracture, the opposite case happens when analyzed from a tension point of view. In the case of tension, less thick specimens reach higher fracture values, this is due to the strain gradient plasticity that we have studied on the previous chapter.

From this data we must notice something; given it´s always the same material, even if the plastic deformation zone varies for each thickness accounting for strain gradient plasticity, this should not happen for the elastic deformation zone as it is governed by the modulus of elasticity (Young Modulus). The reason for this is simple, in a real life lab situation for every repetition of the experiment that is done there will always be a slight change of environment that will lead to slightly different results, perfect reiteration of an experiment is not possible. This proves to be the first hurdle faced when determining this material´s properties, as the young modulus is necessary data to implement in the software. The Young Modulus is calculated from the slope of the elastic zone of the material, the following graphs show repeated iterations of the calculation for the different specimen thickness:

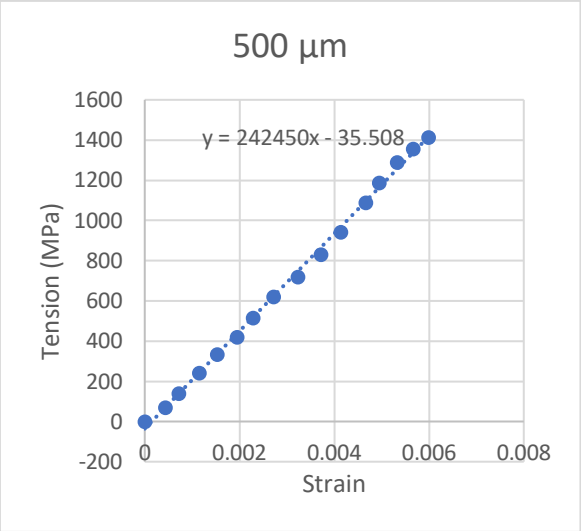

FIGURE 4.8.- Slope of the elastic zone at 500 µm

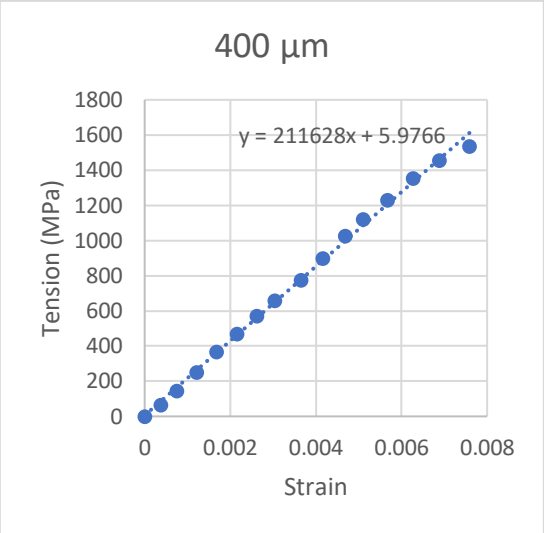

FIGURE 4.9.- Slope of the elastic zone at 400 µm

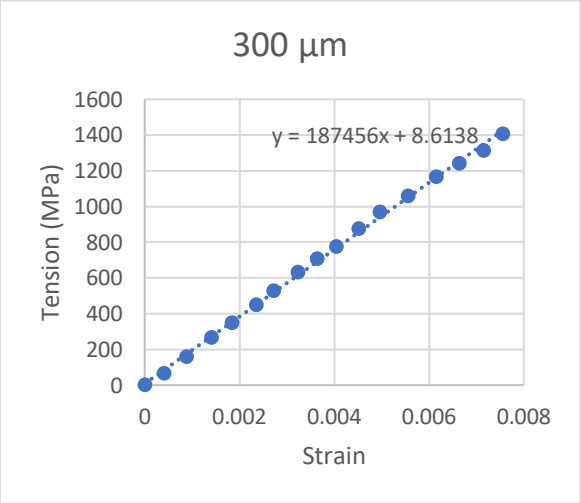

FIGURE 4.10.- Slope of the elastic zone at 300 µm

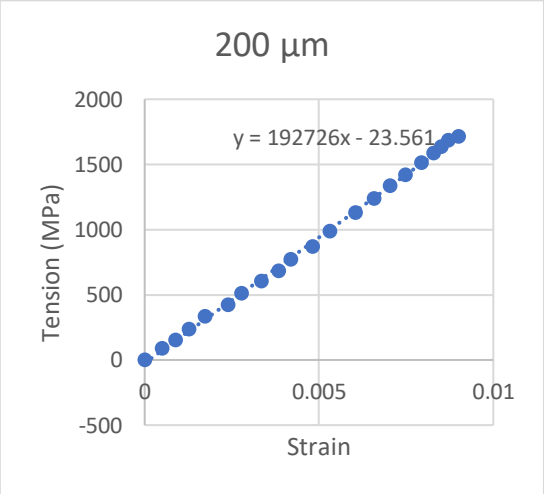

FIGURE 4.11.- Slope of the elastic zone at 200 µm

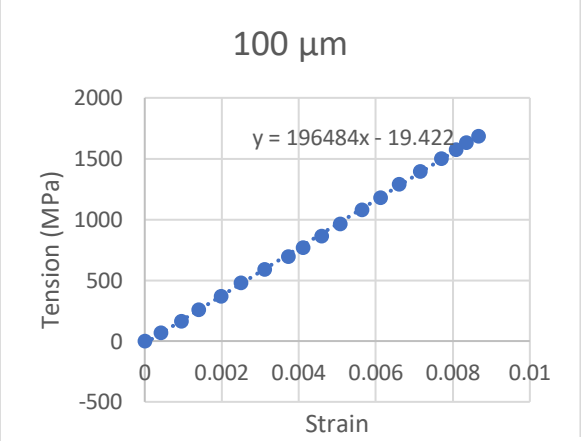

FIGURE 4.12.- Slope of the elastic zone at 100 µm

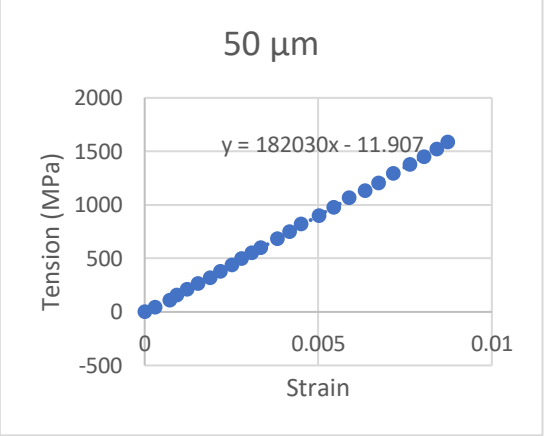

FIGURE 4.13.- Slope of the elastic zone at 50 µm

For the estimated Young Modulus, the average of the previous results was obtained which yielded a modulus of 194064,8 MPa. The reader may be concerned with the estimation approach as we have no guarantee of exactitude, in order to estimate the influence that small changes of the young modulus have in our model different simulations were done in which the only thing that changed was the young modulus for a specimen of 0,5mm thickness:

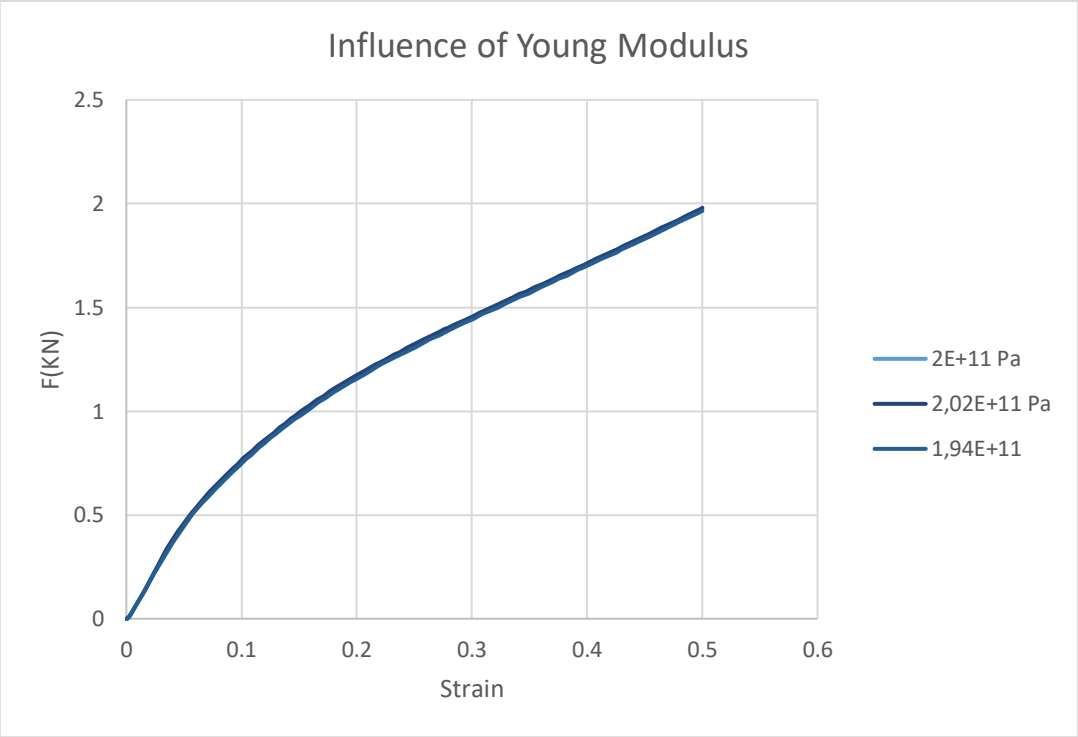

FIGURE 4.14.- Influence of Young modulus in the developed Abaqus model

As the reader can tell, the minor differences in the young modulus don´t lead to huge changes on the nature of the results. We can rest assured with the picked value of 194064 MPa. We can also extract another interesting data from the previous young modulus calculations, when analyzed at room temperature, steel´s young modulus usually ranges from 190 GPa to 220 Gpa, it´s not bold to assume that the material that we are working with is some kind of steel alloy. Because of this we will be setting a common Poisson ratio of 0,25.

Another property of the materials that we shall find is the strain hardening exponent N, it represents the hardening of a material in the forming process and we can kind of

understand it as the "slope" of the plastic region of the stress-strain plot. In order to find it, a logarithmic tension-strain plot is performed for the plastic region of two of the specimens and the slope is then found:

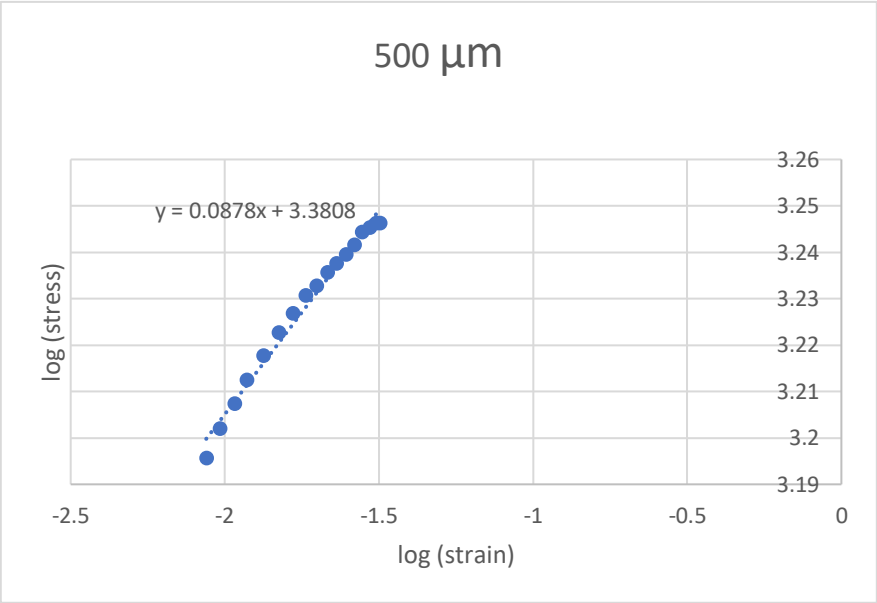

FIGURE 4.15.- Slope of the plastic region for 500µm

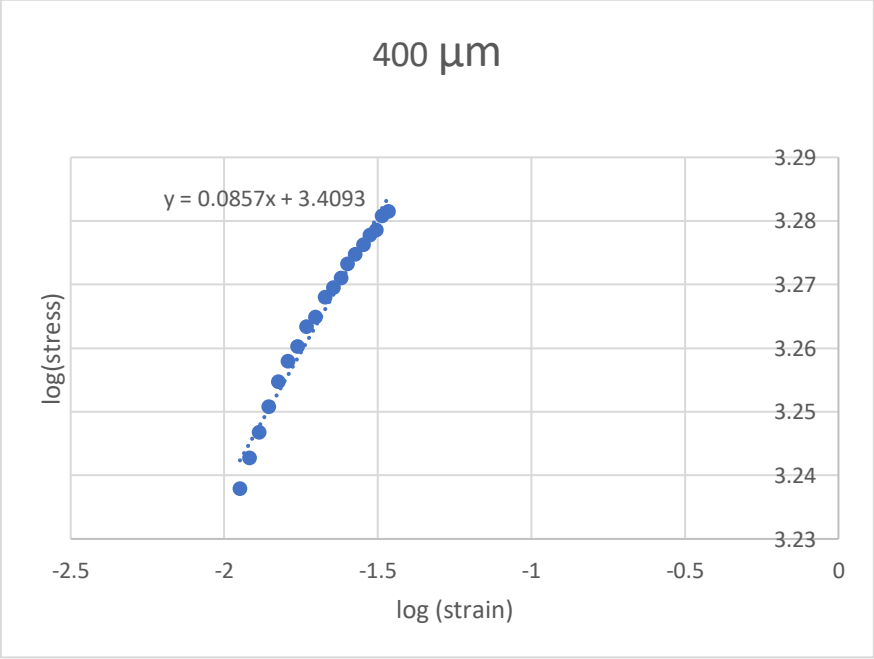

FIGURE 4.16.- Slope of the plastic region for 400 µm

From the graphs we obtain and average N value of 0.09, we shall simplify this value as 0.1 for the sake of simplicity and also to comply with the general rule that metals are found in the 0.1-0.5 range.

Lastly, we need to know the yield stress of the material. This is quite difficult to estimate based purely on the graphs. Theoretically it is considered to be the point of 0,2% strain… but when facing a true case this estimation falls short at delivering accurate results. When observing the stress strain graphs of figure 4.6., we can estimate that the yield stress is at 1400MPa. We shall know if this estimation can be assumed as true when comparing the results offered by the model to the reality, if there is a correlation of results then it´s quite reasonable to say that the estimation was accurate.

4. 5.- CALCULATION PROCESS

The following figures represent the simulation of Abaqus when calculating the reaction force and displacement experienced at the punch when penetrating the specimen (0,5 mm thickness in the particular case shown) at constant speed:

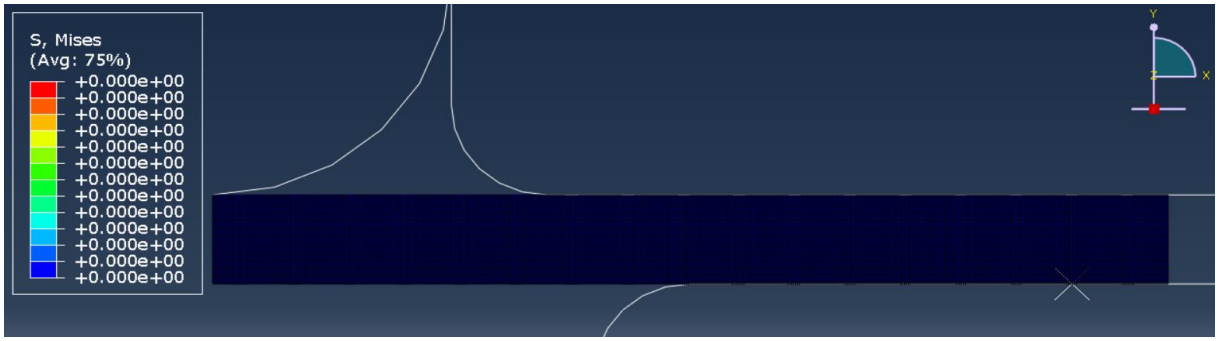

FIGURE 4.17.- Simulation at t=0

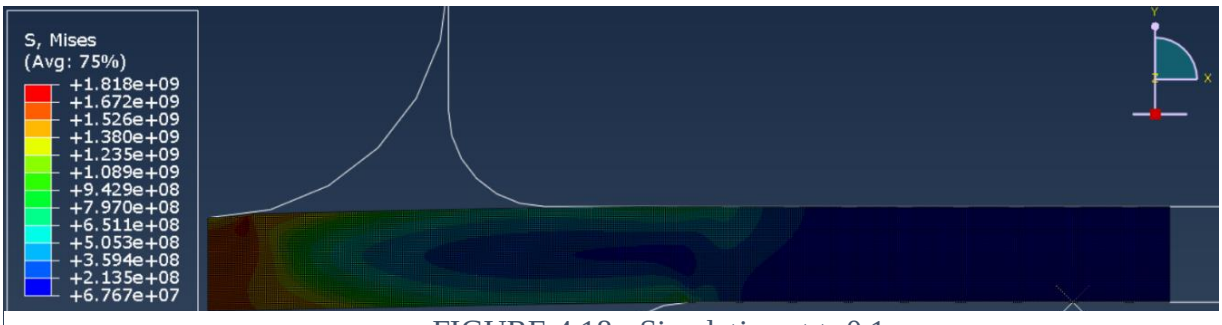

FIGURE 4.18.- Simulation at t=0.1

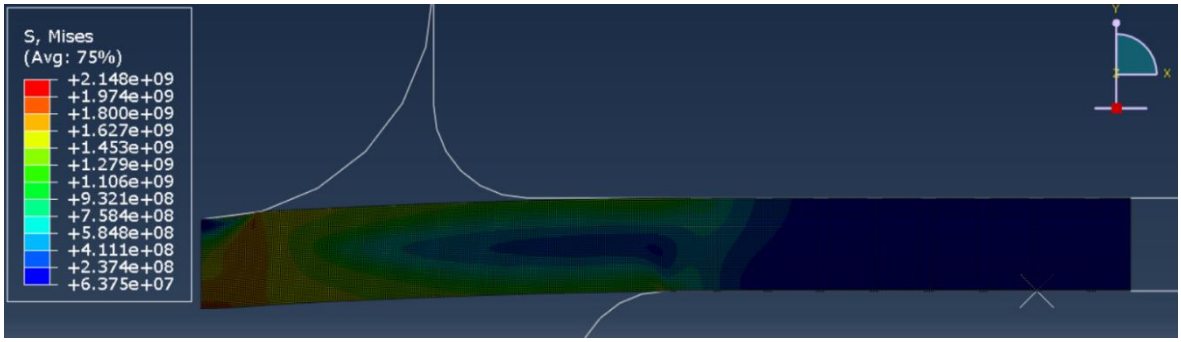

FIGURE 4.19.- Simulation at t=0.2

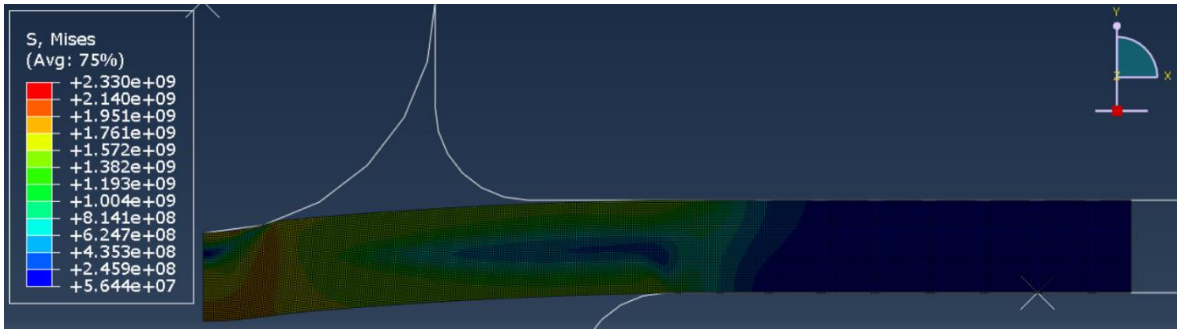

FIGURE 4.20.- Simulation at t=0.3

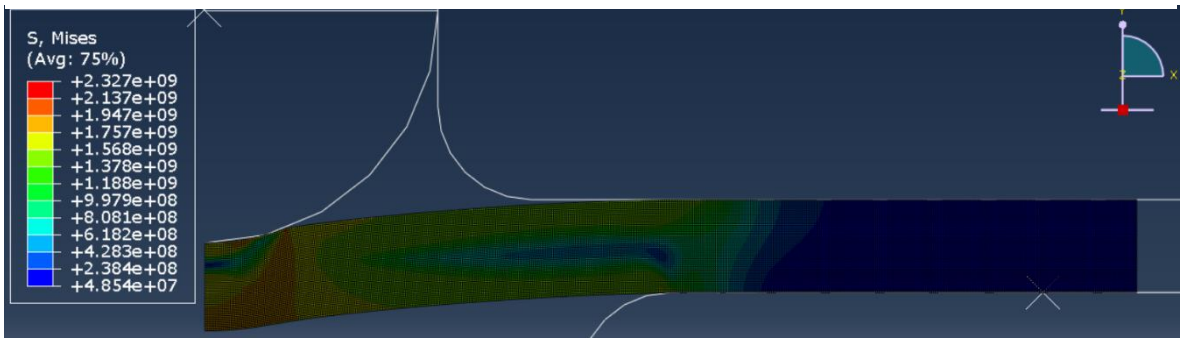

FIGURE 4.21.- Simulation at t=0.4

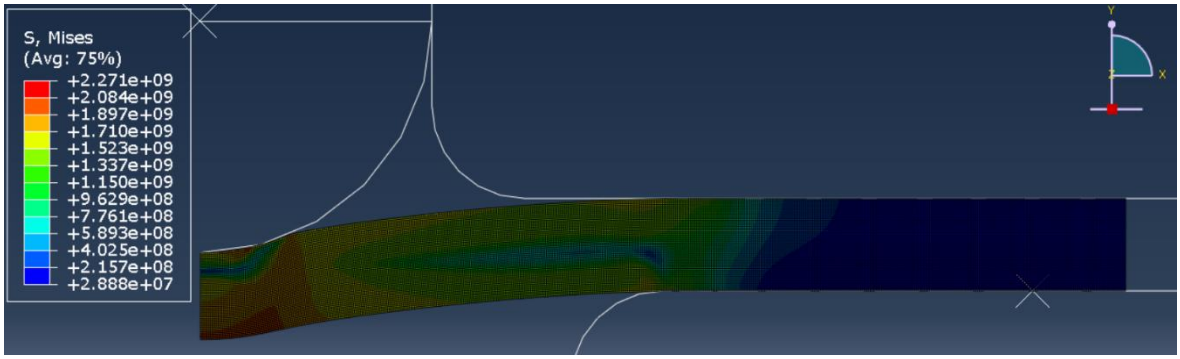

FIGURE 4.22.- Simulation at t=0.5

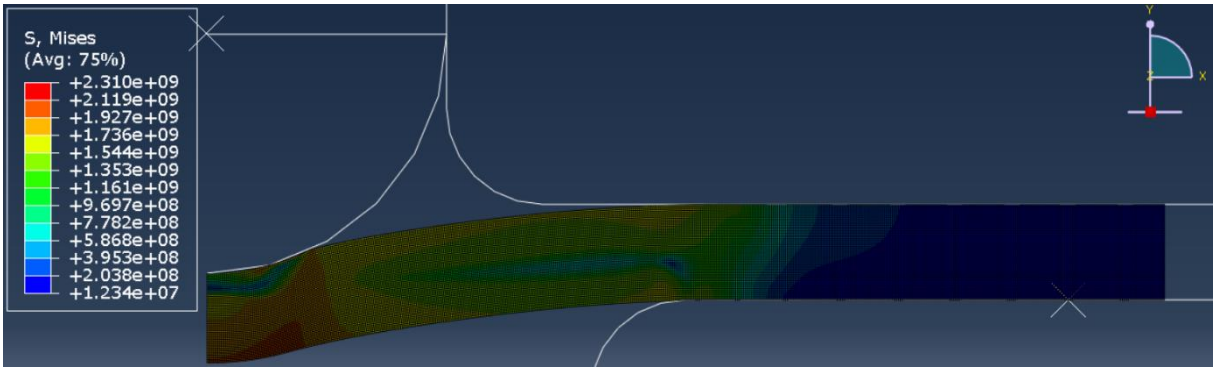

FIGURE 4.23.- Simulation at t=0.6

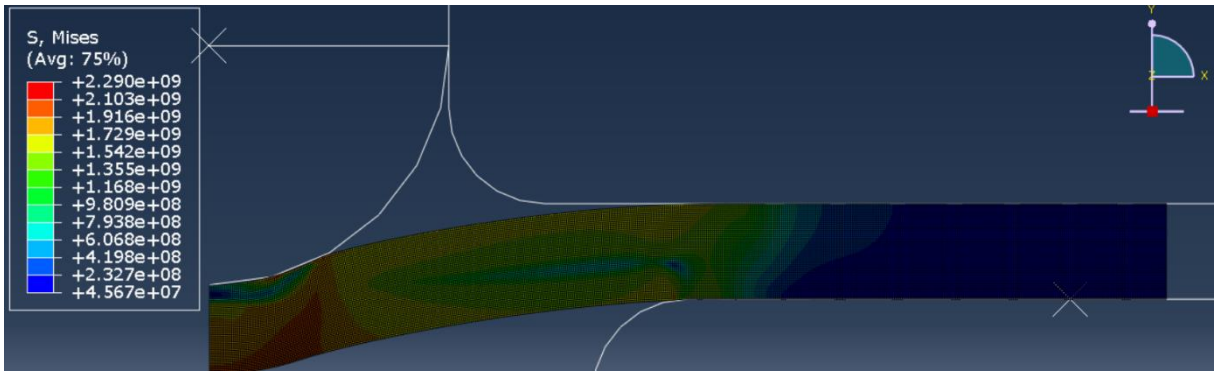

FIGURE 4.24.- Simulation at t=0.7

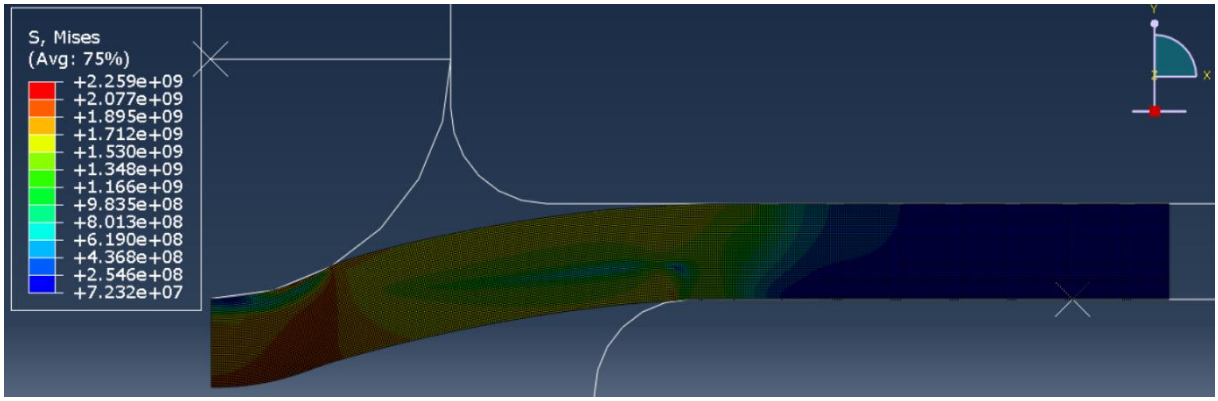

FIGURE 4.25.- Simulation at t=0.8

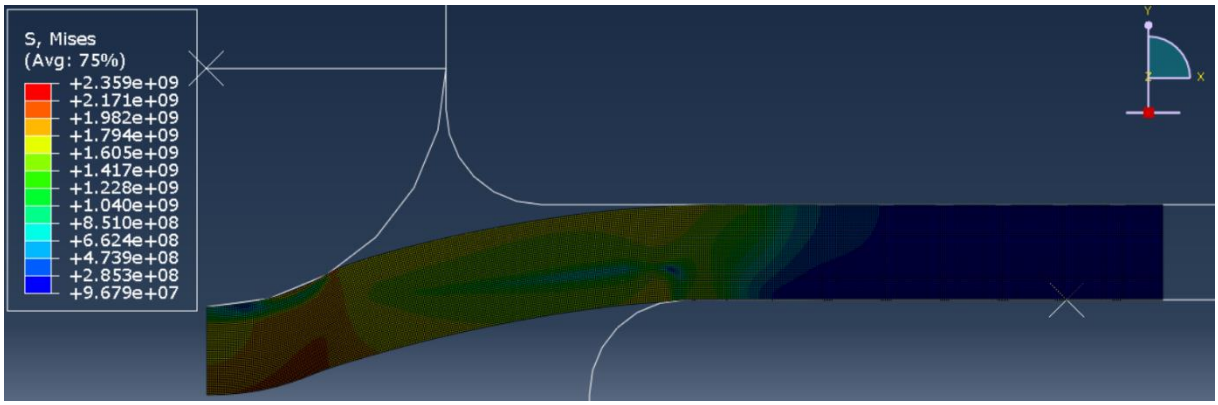

FIGURE 4.26.- Simulation at t=0.9

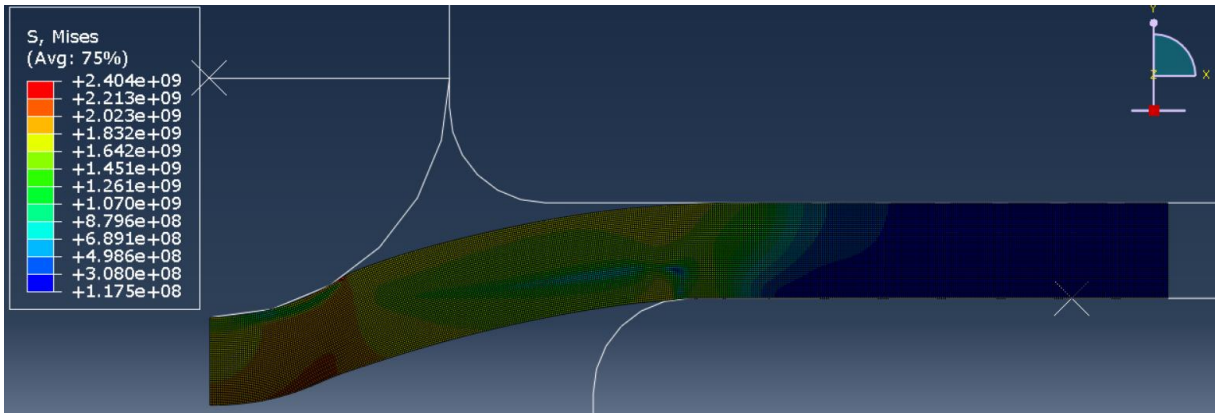

FIGURE 4.27.- Simulation at t=1

Even though the images are descriptive of the process, they can´t provide us with the data we need to obtain from each case. For that we have set a reference point on top of the punch (represented as a white X) and we will obtain both data on the reaction force and the displacement experienced on this point related to time:

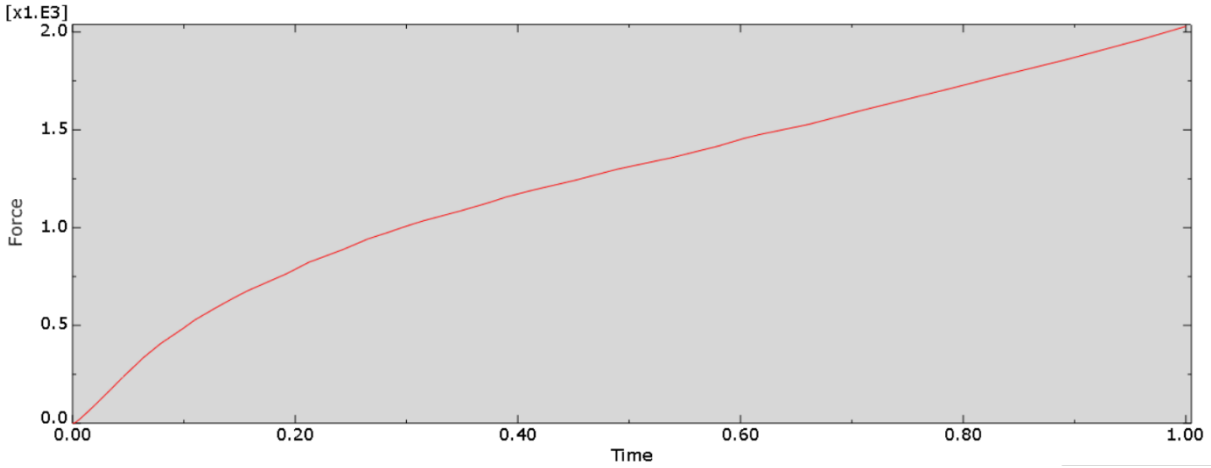

FIGURE 4.28.- Results of the reaction force vs time

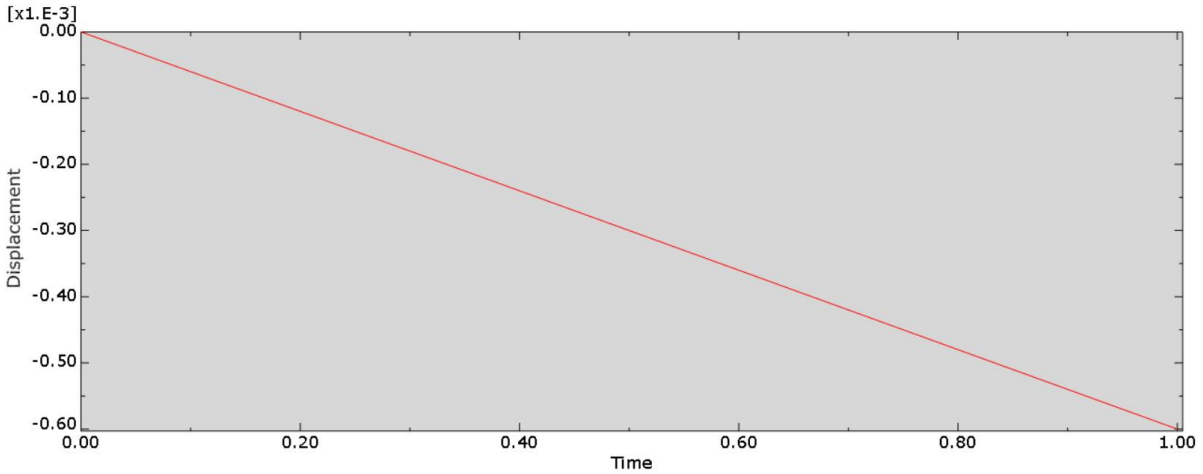

FIGURE 4.29.- Results of displacement vs time

By using Abaqus to combine both graphs we will get a plot that relates reaction force vs. displacement:

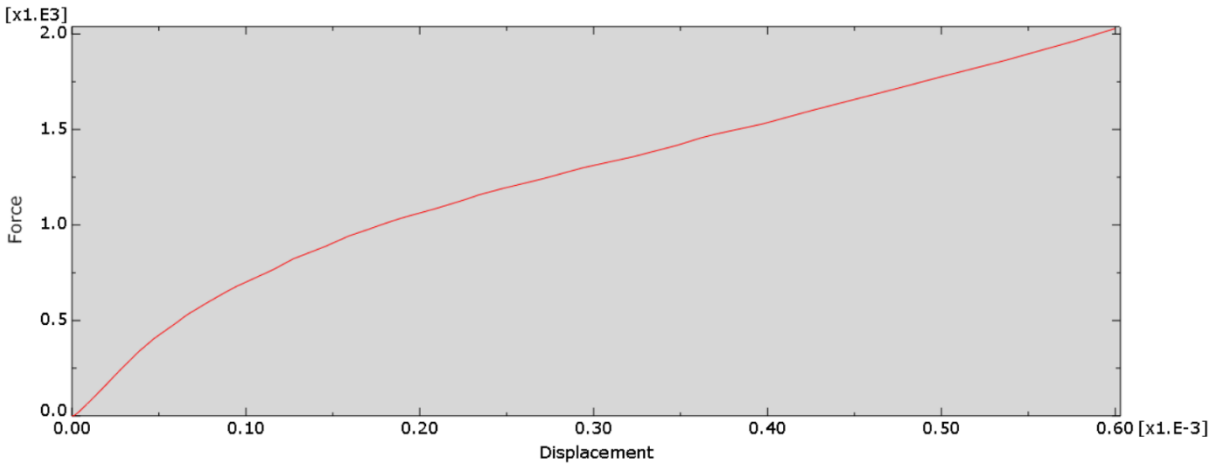

FIGURE 4.30.- Plot of the force vs displacement by combining both previous graphs

This process will be repeated successively with different specimen thickness but preserving the same material properties, this way we will obtain the data that will be useful for comparing the behavior. This data will then be exported to Excel in order to be able to display all iterations of the experiment on the same graph and then compare it to the lab results.

4.6.- RESULTS AND ANALYSIS

At this point we need to go back to figure 4.7. as it will be our reference to evaluate whether the results we are obtaining are adjusted to reality. Following the procedure explained in the previous section, the results the software provide for different thickness can be represented in the following graph:

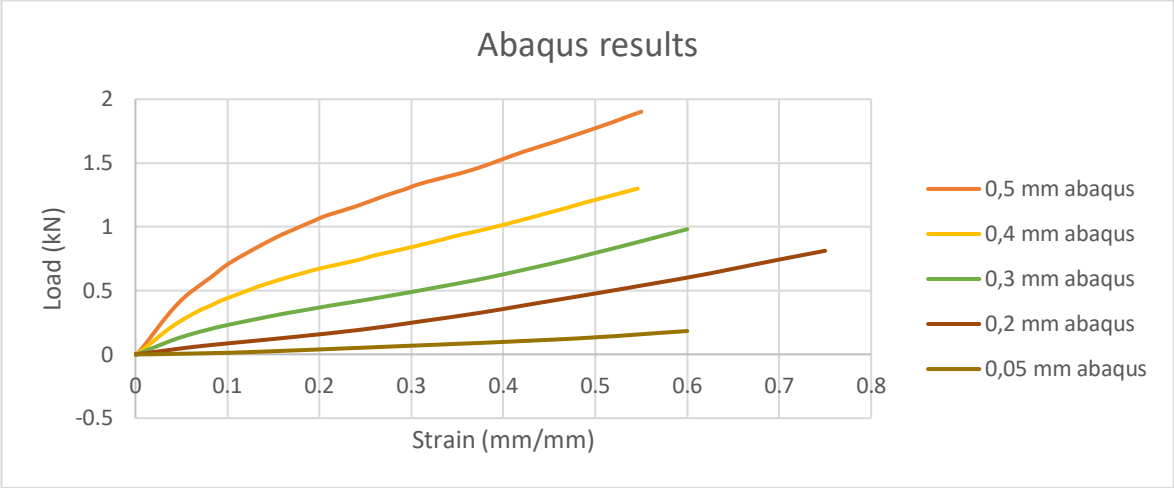

FIGURE 4.31.- Abaqus results at different thickness

Comparing with the lab results considering there is a minor slip at the beginning of the lab experiment we get the following relationships between lab and our model

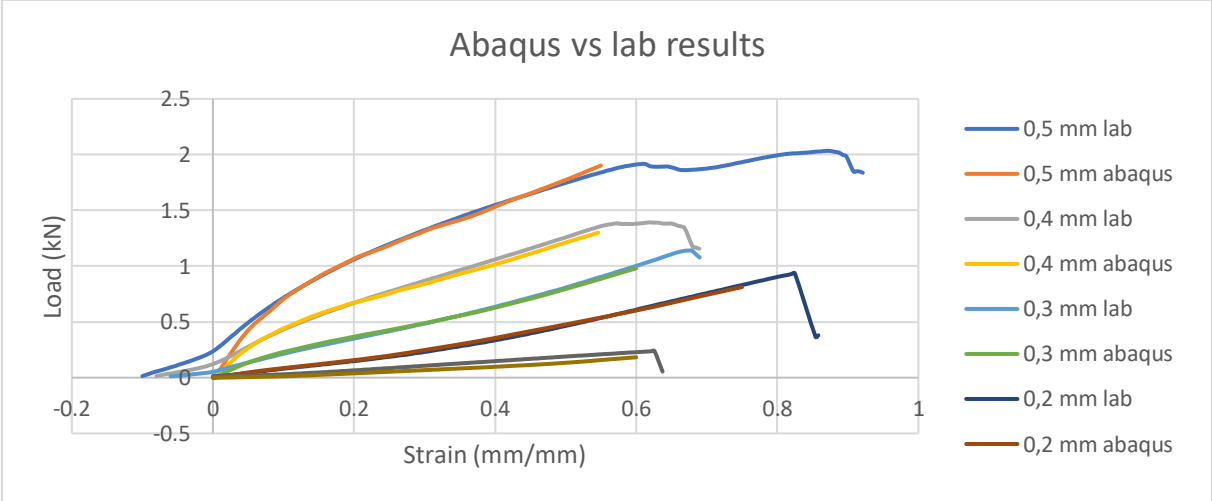

FIGURE 4.32.- Abaqus results vs lab results at different thickness

It is important to understand why the Abaqus results do not match the lab results until the very end, the reason for this is that there is no implementation of fracture mechanism for the software within the scope of this study.

In order to evaluate size effects, we need to apply a relationship that should, if the size effect doesn't exist, give out the same relationship for each of the experiments. We can tackle this on a set of different ways but the objective will remain the same: we need to stablish a relationship that will dimensionless the results. For that we will multiply the strain times the thickness to the power of three for each of the experiments:

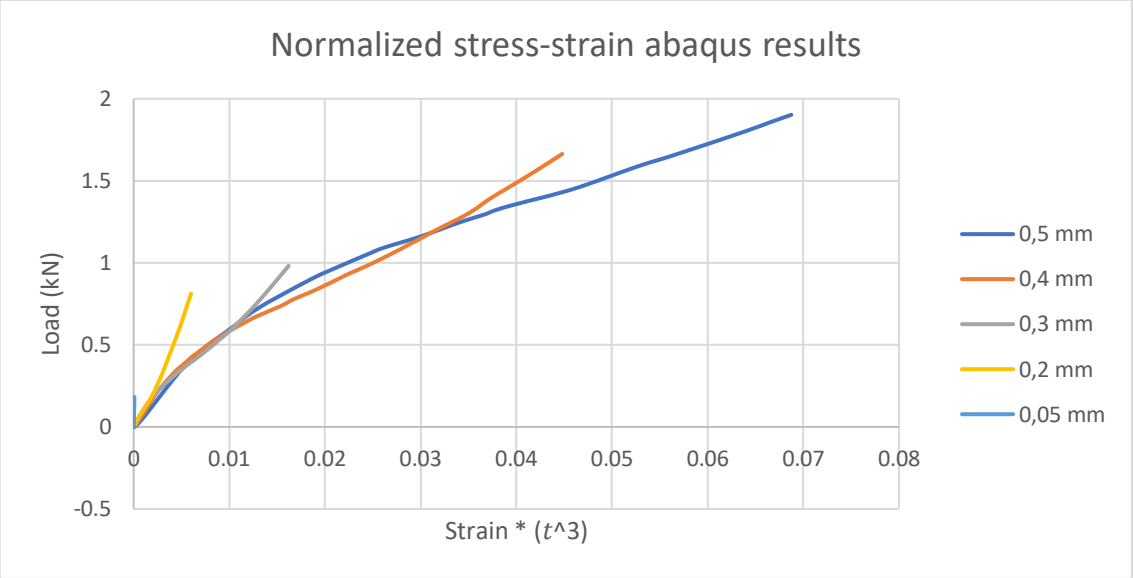

FIGURE 4.33.- Normalized stress-strain Abaqus results

As we see on the graph there is a considerable difference on the experimental results at different thickness even if we dimensionless the results. This is due to the strain gradient plasticity and goes to prove that our model correctly considers its effects and applies it to the model. In order to see if the size effect in Abaqus is proportional to the one found in reality we can plot the normalized lab results taking into account the before mentioned slip at the beginning of the experiment on the same graph:

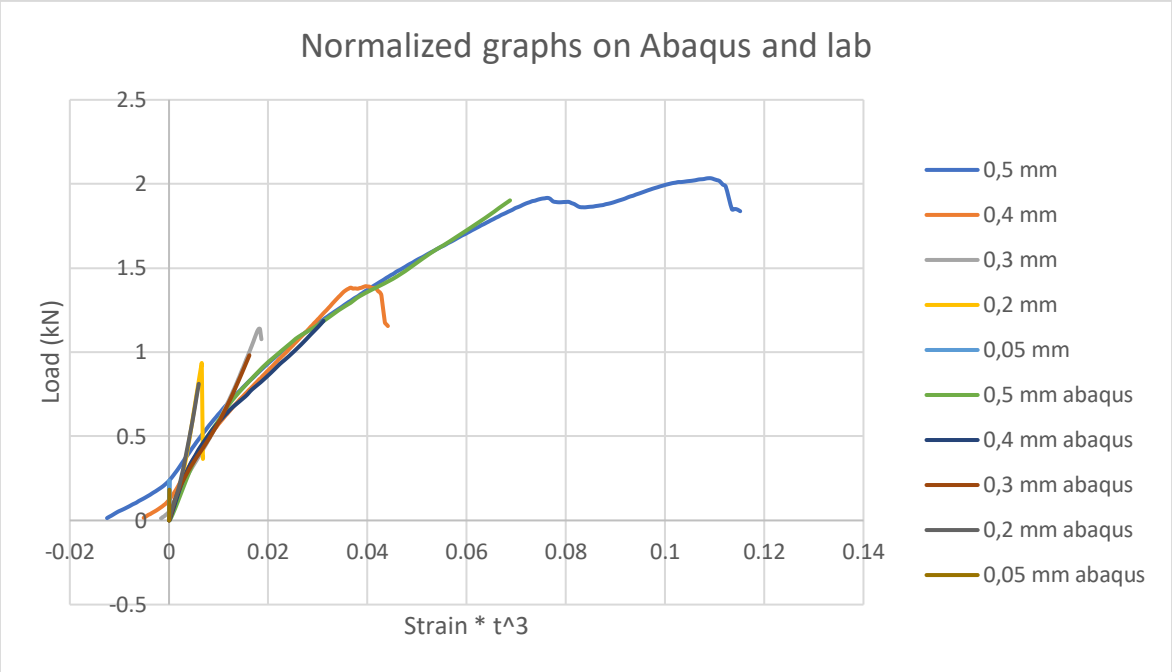

FIGURE 4.34.- Normalized graphs on Abaqus vs lab

Finally, we see that the normalized lab results give out for similar results to the one obtained through Abaqus, not only the size effect is seen through our model, we can also say that the results are accurate compared to reality

CHAPTER 5

5.- Conclusions

Having concluded the results of this paper. The following conclusions and reflections can be extracted from this work:

1. A successful model for the Small Punch Test has been developed for Abaqus, the use of axisymmetric allows for an efficient model that has proven to give accurate results while preserving speed of calculation.

2. The size effect of strain gradient plasticity has been thoroughly analyzed through Abaqus results and comparison of them to the lab results. As a result, it´s clear that the effect exists and that we have enough evidence to justify that the developed model not only proves the existence, it also provides reliable results with a close relationship to the real ones.

3. The effect of the implemented UMAT (User material) subroutine has been proven, allowing us to obtain a size effect analysis on Abaqus even if the base program does not consider it. Subroutines will allow us to introduce desired effects into the program allowing us practically unlimited types of analysis.

4. We have been successful at determining the material properties from the results of lab experiments on its stress/load-strain relationships. The utility of this kind of experiments is proven as it allows to know a lot of information on the studied material with a minor effort both in terms of work and resources.

5. For future works, I trust that there is more potential to the developed model, given it has proved reliable at describing plastic deformation and size effects it would be

interesting to implement a fracture mechanism and evaluate the reliability of the software and subroutine when predicting fracture points and strength.

6.- Bibliography

1. Zhengyi Jiang, Jingwei Zhao and Haibo Xie: *Microforming technology: theory, simulation and practice*. ACADEMIC PRESS. 2017

2. **N.A. Fleck, G.M. Muller, M.F. Ashby and J.W. Hutchinson:** *Strain gradient plasticity: Theory and experiment.* PERGAMON PRESS LTD. 1993

3. Lorraine F: *Materials processing: A Unified Approach to Processing of Metals, Ceramics and Polymers. ACADEMIC PRESS LTD.* 2015

4. Vazquez Briseño: *Teoría de la plasticidad. AZCAPOTZALCO.* 2017

5. D.W.A. Rees: *Basic engineering plasticity*. ELSEVIER. 2012

6. Pelleg Joshua: *Mechanical properties of materials.* SPRINGER SCIENCE & BUSINESS MEDIA. 2012

7. R.E. Smallman, A.H.W. Ngan: *Modern physical metallurgy*. ELSEVIER. 2014

8. J.P. Mercier, G. Zambelli, W. Kurtz: *Introduction to materials science.* ELSEVIER. 2012

9. E. Alarcón, M. Doblaré: *Teoría de plasticidad*. UNIVERSIDAD POLITÉCNICA DE MADRID

10. F.J. Belzunce Varela, J.A. Viña Olay: *Fundamentos de ciencia de los materiales*. UNIVERSIDAD DE OVIEDO

11. G. Z. Voyiadjis, Y. Song: *Strain gradient continuum plasticity theories: Theoretical, numerical and experimental investigations.* ELSEVIER. 2019

12. A.G. Evans, J.W. Hutchsinson: *A critical assessment of theories of strain gradient plasticity.* ELSEVIER. 2009

13. L.F. Francis: *Materials processing*. ACADEMIC PRESS. 2015

14. J. Massa, J. Giro and A. Giudici: *Compendio de cálculo structural II.* UNIVERSIDAD NACIONAL DE CÓRDOBA. 2017

15. P. Prat: *Elasticidad y plasticidad*. UNIVERSIDAD POLITÉCNICA DE CATALUÑA. 2006

16. M.D. Hayes, D.B. Edwards, A.R. Shah: *Fractography in failure analysis of polymers.* ELSEVIER. 2015

17. E. Martínez-Pañeda: *ABAQUS implementation of the conventional mechanism-based strain gradient plasticity theory.* TECHNICAL UNIVERSITY OF DENMARK. 2015

18. E. Martínez-Pañeda, I.I. Cuesta, I. Peñuelas, A. Díaz, J.M. Alegre: *Damage modeling in small punch test specimens.* ELSEVIER. 2016

19. ABAQUS: *User´s guide*. 2016

20. ABAQUS: *Theory guide*. 2016